The Plant Cell, Vol. 25: 4209–4226, October 2013, www.plantcell.org

A Mediator of Singlet Oxygen Responses in *Chlamydomonas reinhardtii* and *Arabidopsis* Identified by a Luciferase-Based Genetic Screen in Algal Cells[W]

Ning Shao,[1] Guang You Duan, and Ralph Bock[2]

Max-Planck-Institut für Molekulare Pflanzenphysiologie, 14476 Potsdam-Golm, Germany

ORCID ID: 0000-0001-7502-6940 (R.B.).

All cells produce reactive oxygen species (ROS) as by-products of their metabolism. In addition to being cytotoxic, ROS act as regulators of a wide range of developmental and physiological processes. Little is known about the molecular mechanisms underlying the perception of ROS and initiation of cellular responses in eukaryotes. Using the unicellular green alga *Chlamydomonas reinhardtii*, we developed a genetic screen for early components of singlet oxygen signaling. Here, we report the identification of a small zinc finger protein, METHYLENE BLUE SENSITIVITY (MBS), that is required for induction of singlet oxygen–dependent gene expression and, upon oxidative stress, accumulates in distinct granules in the cytosol. Loss-of-function *mbs* mutants produce singlet oxygen but are unable to fully respond to it at the level of gene expression. Knockout or knockdown of the homologous genes in the higher plant model *Arabidopsis thaliana* results in mutants that are hypersensitive to photooxidative stress, whereas overexpression produces plants with elevated stress tolerance. Together, our data indicate an important and evolutionarily conserved role of the MBS protein in ROS signaling and provide a strategy for engineering stress-tolerant plants.

INTRODUCTION

Phototrophic organisms produce a range of different reactive oxygen species (ROS) either by energy transfer or electron transfer reactions. While electron transfer produces superoxide (O_2^-) radical ions that subsequently can be converted to hydrogen peroxide (H_2O_2) or hydroxyl radicals, energy transfer to molecular oxygen results in the generation of singlet oxygen ($^1O_2$; Apel and Hirt, 2004). Plant cells produce ROS as unavoidable byproducts of aerobic metabolism, with the photosynthetic electron transport chain being a major source (Mullineaux and Karpinski, 2002; Foyer and Noctor, 2003; Wagner et al., 2004; Mubarakshina et al., 2010). Efficient enzymatic and nonenzymatic detoxification mechanisms are in place to prevent accumulation of excessive amounts of ROS and the resultant oxidative damage to biomolecules, especially proteins and lipids (op den Camp et al., 2003; Apel and Hirt, 2004; Henmi et al., 2004; Scheller and Haldrup, 2005; Krieger-Liszkay and Trebst, 2006). Over the past two decades, it has become increasingly clear that, even under nonstressed conditions, plants continuously produce ROS and that ROS do not merely act as cytotoxic agents, but also can be employed as signaling molecules. In vascular plants, ROS signaling has been implicated in a variety of physiological and developmental processes, including pathogen defense, abscisic acid–induced stomatal closure, maintenance of ion homeostasis, root development and gravitropism, as well as retrograde signaling from organelles to the nucleus (Lam et al., 2001; Apel and Hirt, 2004; Fischer et al., 2007; Pogson et al., 2008; Galvez-Valdivieso and Mullineaux, 2010; Jaspers and Kangasjärvi, 2010; Tsukagoshi et al., 2010; Jiang et al., 2012).

$^1O_2$ is produced mainly by photosystem II (PSII), especially upon absorption of excess light energy (Krieger-Liszkay and Trebst, 2006). It is generated via energy transfer from the triplet state of chlorophyll in the PSII reaction center to molecular oxygen in its ground state ($^3O_2$). Release of $^1O_2$ results in the rapid induction of the expression of a specific set of nuclear genes (including transcription factors), as elegantly revealed by genetic studies in the conditional *Arabidopsis thaliana* mutant *fluorescent* (*flu*; op den Camp et al., 2003; Laloi et al., 2007; Kim et al., 2009). This mutant accumulates high levels of the photosensitizer protochlorophyllide in the dark and, following a shift to the light, produces massive amounts of $^1O_2$. Interestingly, the resulting growth arrest and cell death responses are not directly caused by $^1O_2$ toxicity but result from a genetic program (that is dependent on the EXECUTER proteins; Wagner et al., 2004; Lee et al., 2007; Kim et al., 2012).

Apart from the $^1O_2$-mediated cell death pathway, only a few components of the cellular machinery involved in $^1O_2$ sensing and signaling have been identified to date. Recent biochemical work has demonstrated that carotenoid oxidation products (especially β-cyclocitral) act as oxidative stress signals that mediate responses to $^1O_2$ in higher plants, including the early transcriptional responses at the level of nuclear gene expression (Ramel et al., 2012a). In addition, several protein factors, including a bZIP-type putative transcription factor (apparently specific to green algae; Fischer et al., 2012) and a member of the P-subunit of photosystem II family (Brzezowski et al., 2012), have been implicated in $^1O_2$ signaling. However, what connects $^1O_2$ and/or the primary chemical signals generated by $^1O_2$ (oxidized carotenoids

[1] Current address: South China Botanical Garden of the Chinese Academy of Sciences, Guangzhou 510650, China.
[2] Address correspondence to rbock@mpimp-golm.mpg.de.
The author responsible for distribution of materials integral to the findings presented in this article in accordance with the policy described in the Instructions for Authors (www.plantcell.org) is: Ralph Bock (rbock@mpimp-golm.mpg.de).
[W] Online version contains Web-only data.
www.plantcell.org/cgi/doi/10.1105/tpc.113.117390

and, perhaps, oxidized lipids; Fischer et al., 2012; Ramel et al., 2012a) with the early transcription factors mediating the downstream changes in gene expression, is currently unknown. It is conceivable that sensor proteins monitor the levels of $^1O_2$ either directly or indirectly by measuring the concentration of reaction products generated at or close to the site of $^1O_2$ production. A better understanding of the molecular mechanisms of $^1O_2$ sensing, signaling, and detoxification is not only relevant to basic research, but also is essential for improving the tolerance of crops plant to photooxidative stress conditions.

The unicellular green alga *Chlamydomonas reinhardtii* has become a useful model organism for a wide range of biological questions. It combines a powerful classical genetics with the availability of excellent genetic and genomic resources. The completion of the *C. reinhardtii* genome sequencing project (Merchant et al., 2007) along with the development of new molecular tools (Schroda et al., 2000; Shao and Bock, 2008; Neupert et al., 2009; Ramundo et al., 2013) made it possible to conduct reporter gene-based genetic screens for new components of signal transduction pathways, including ROS signaling (Fischer et al., 2010, 2012; Brzezowski et al., 2012).

Here, we combined a previously developed sensitive reporter of gene expression in *C. reinhardtii* (Shao and Bock, 2008) with a previously characterized ROS-responsive promoter (Shao et al., 2007) and an efficient insertional mutagenesis strategy (Gonzalez-Ballester et al., 2011) to set up a new screen for algal mutants defective in early cellular $^1O_2$ responses. We report the identification of a small zinc finger protein (METHYLENE BLUE SENSITIVITY [MBS]) that plays a crucial role in mediating $^1O_2$-responsive gene expression in *C. reinhardtii*. Importantly, characterization of the homologous genes in the higher plant model *Arabidopsis* revealed a critical role of the MBS proteins in mediating $^1O_2$ signaling and determining oxidative stress tolerance, indicating evolutionary conservation of the pathway from green algae to vascular plants.

RESULTS

A Genetic Screen for ROS Signaling Mutants in *C. reinhardtii*

We previously reported that a codon-optimized version of the luciferase gene from the copepod *Gaussia princeps* provides a sensitive reporter of gene expression in the unicellular model alga *C. reinhardtii* (Shao and Bock, 2008). The availability of a sensitive reporter gene has opened up the possibility to exploit the convenience of *C. reinhardtii* genetics for the isolation of regulators of gene expression by forward genetics. This provides a particularly attractive alternative to higher plant models, where complex multicellular organization makes mutant screens difficult or impossible. Light stress–induced ROS signaling is a case in point because the primary responses are largely confined to photosynthetically active tissues and therefore affect only a small number of the many cell types present in higher plants.

We used the codon-optimized *G. princeps* luciferase gene in combination with the $^1O_2$-responsive P_{HSP70A} promoter (Shao et al., 2007) to set up a genetic screen for mutants defective in $^1O_2$ sensing and/or signaling (Figure 1A). To this end, an algal strain harboring the P_{HSP70A}-driven reporter cassette was subjected to large-scale insertional mutagenesis based on random insertion of a hygromycin resistance gene cassette (Berthold et al., 2002; Figure 1A). A total of 4890 insertion mutants were generated by transformation and screened for their inability to induce luciferase expression in response to $^1O_2$ stress. $^1O_2$ stress was applied by exposure of algal cultures to methylene blue (MB), a photosensitizer that is readily taken up by *C. reinhardtii* cells and triggers the production of $^1O_2$ in the light (Shao et al., 2007). Seventeen mutants were identified that lacked luciferase induction upon application of $^1O_2$ stress (Figure 1B). To distinguish between mutants that are specifically defective in their response to $^1O_2$ and mutants with general defects in expression of the luciferase reporter, heat stress experiments were performed. The *HSP70A* promoter driving the luciferase reporter is not only responsive to $^1O_2$, but it is also strongly inducible by heat shock. As the heat response is genetically distinct from the response to $^1O_2$ (Shao et al., 2007; Lodha et al., 2008; Shao and Bock, 2008), any mutant specifically affected in $^1O_2$ responses should still show wild-type-like luciferase induction by heat. This was the case for 12 of the algal mutants identified in the MB screen (Figure 1C), suggesting that these 12 mutants are neither generally affected in luciferase expression nor generally defective in their response to abiotic stresses.

Identification of the *MBS* Gene

The algal mutants for the genetic screen were generated by insertional mutagenesis to facilitate identification of the mutated gene based on tagging with the selectable marker gene cassette (Figure 1A). However, previous work has shown that only ~50% of the mutations are tagged by the transforming DNA (Dent et al., 2005). Moreover, the integration of transforming DNA into the *C. reinhardtii* nuclear genome is often accompanied by larger deletions at the site of insertion, thus additionally complicating gene identification. When isolation of flanking sequences by inverse PCR was attempted for four of the mutants that proved to be $^1O_2$ specific, only one of the mutants (P45E1; Figures 1B and 1C) turned out to be tagged and was devoid of a genomic deletion accompanying marker insertion. The mutant harbored a single-copy insertion of the hygromycin resistance cassette in the putative promoter region of a small gene of unknown function (insertion site: chr_9:4592978-4593500; Joint Genome Initiative *C. reinhardtii* genome version 4.0). The gene, subsequently referred to as *MBS* (Figure 1D) is interrupted by three introns, as revealed by comparison of the genomic sequence with a full-length clone in the expressed sequence tag (EST) database and further confirmed by RT-PCR and DNA sequencing (Figure 1E). RT-PCR assays also indicated that the insertion of the hygromycin cassette into the promoter completely abolishes *MBS* expression in the isolated *mbs* mutant (Figures 1D and 1E), suggesting that the mutant represents a null allele.

To confirm that the tagged locus is indeed responsible for the mutant phenotype, the mutant strain was complemented by genetic transformation with a cDNA expression construct. The resulting transgenic strains (P_{PsaD}:*MBS*/*mbs*) showed wild-type-like tolerance to MB under conditions where the *mbs* mutant died, presumably due to lethal photooxidative damage (Figure 1F).

The putative MBS protein is a small protein of 10.7 kD. It has homologs in all lineages of land plants. While it is encoded by

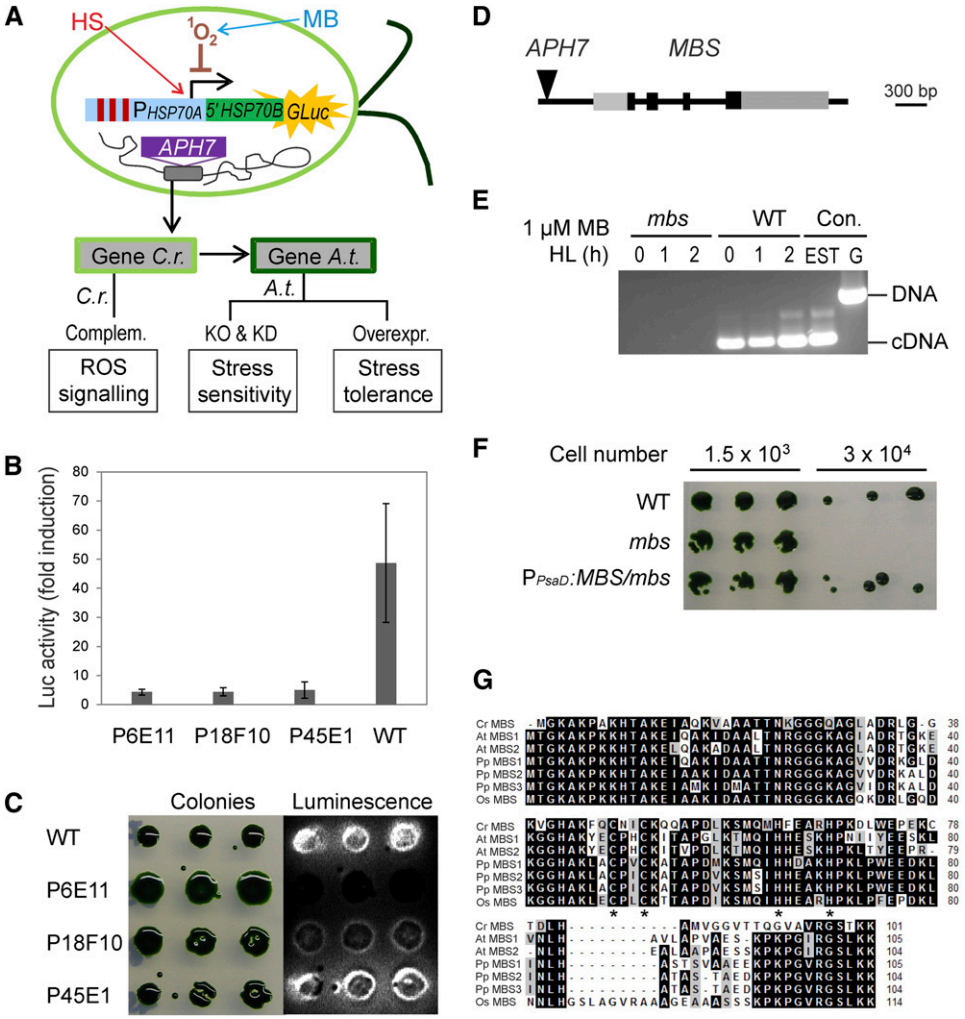

Figure 1. Screen for ROS Signaling Mutants in *C. reinhardtii* and Identification of the *MBS* Gene.

(A) Schematic overview of the experimental strategy for isolating regulators of ROS signaling. High-throughput genetic screens with a ROS-inducible reporter gene in *C. reinhardtii* are combined with reverse genetic analyses in *Arabidopsis*. An algal strain expressing a $^1O_2$-inducible luciferase reporter gene (P_{HSP70A}-*5′HSP70B-GLuc*; Shao and Bock, 2008) was subjected to insertional mutagenesis with the hygromycin resistance gene *APH7* (Berthold et al., 2002). Screening for mutants defective in $^1O_2$-mediated signaling was performed by treatment of cultures with the photosensitizer MB that generates $^1O_2$ in the light. As the *HSP70A* promoter also responds to heat stress (HS; heat stress elements indicated as red bars), ROS signaling mutants can be identified as strains displaying luciferase induction upon heat stress, but lacking induction upon exposure to $^1O_2$ stress. Assays performed on mutants and transgenic lines are indicated in the boxes at the bottom of the panel. *C.r.*, *C. reinhardtii*; *A.t.*, *Arabidopsis*; Complem., complementation; KO, knockout; KD, knockdown; Overexpr., overexpression.

(B) Example of three insertion mutants (P6E11, P18F10, and P45E1) that do not respond to $^1O_2$ stress generated by HL (1000 µE m^{-2} s^{-1}) in the presence of 1 µM MB (monitored by luciferase bioluminescence). Data are mean values ± SD of three biological replicates. WT, wild type.

(C) Heat stress response in the three insertion mutants P6E11, P18F10, and P45E1. Growing algal colonies were shifted from 23 to 40°C for 1 h. While the P45E1 mutant has a normal heat stress response (as evidenced by induction of luciferase luminescence), the P6E11 and P18F10 mutants show an impaired response to heat stress compared with the wild type.

(D) Model of the *MBS* gene and insertion site of the *APH7* marker in the *mbs* mutant of *C. reinhardtii*. Black boxes represent exons, and gray boxes represent 5′ and 3′ untranslated regions as confirmed by EST sequencing.

(E) RT-PCR analysis demonstrating the absence of *MBS* transcripts in mutant P45E1 (*mbs*). The 300-bp *MBS* gene-specific RT-PCR product is obtained with wild-type cDNA as template after 0, 1, and 2 h of HL treatment (1000 µE m^{-2} s^{-1}) in the presence of 1 µM MB but cannot be amplified from cDNA of the *mbs* mutant. PCR products amplified from an EST clone (AV621044) and genomic DNA (G) of the wild type are shown as controls (Con.).

(F) MB-sensitive phenotype of the *mbs* mutant (P45E1) compared with the wild type and the complemented P_{PsaD}:*MBS*/*mbs* strain.

(G) Alignment of the amino acid sequences of the MBS proteins from the alga *C. reinhardtii* (Cr), the moss *P. patens* (Pp), and the higher plants *Arabidopsis* (At) and rice (Os). Putative MBS sequences were retrieved from the full genome sequences and the alignment was produced using BioEdit (http://www.mbio.ncsu.edu/bioedit/bioedit.html). The asterisks indicate the zinc finger motif of the C_2H_2 type. Amino acids highlighted in black indicate identical residues in all sequences, and residues in gray denote similar amino acids.

a single-copy nuclear gene in *C. reinhardtii* and rice (*Oryza sativa*), two (highly similar) copies are found in the *Arabidopsis* genome and three copies in the genome of the model moss *Physcomitrella patens* (Figure 1G). The only salient feature identifiable upon bioinformatics analysis of the amino acid sequence was a single zinc finger motif of the C_2H_2 type (Figure 1G).

Isolation and Characterization of *mbs* Mutants in *Arabidopsis*

To assess the possible involvement of the *MBS* homologs in $^1O_2$ sensing and/or signaling in embryophytes, we sought to isolate mutants of the two genes in *Arabidopsis*, tentatively named *MBS1* (AT3G02790) and *MBS2* (AT5G16470). Neither of the two genes displays a pronounced tissue-specific or developmental stage-specific expression pattern, with the exception of a moderate upregulation of *MBS2* during senescence, a condition known to involve substantial production of ROS (see Supplemental Figure 1 online).

Searches of the collections of T-DNA–tagged *Arabidopsis* lines revealed three candidate mutants, two of them harboring insertions upstream of *MBS1* (*mbs1-1* and *mbs1-2*) and one carrying a T-DNA insertion upstream of *MBS2* (*mbs2-1*; Figure 2A). Sequencing of the insertion sites confirmed the location of the T-DNA inserts. To determine the effects of the T-DNA insertions on *MBS* expression, homozygous mutant lines were isolated and analyzed by nonquantitative RT-PCR assays. The results revealed that, while the *mbs1-1* mutant showed no detectable expression and therefore is probably equivalent to a knockout mutant, the *mbs1-2* and *mbs2-1* mutants had wild-type-like expression levels (Figure 2B). This finding is consistent with the T-DNA insertion in the *mbs1-1* mutant being much closer to the coding region than in the other two mutants (Figure 2A).

The *mbs1-1* mutant did not display a discernible phenotype under standard growth conditions. To preliminarily test for involvement of *Arabidopsis MBS1* in plant responses to $^1O_2$, the sensitivity of *mbs1-1* mutant plants to high-light (HL) stress was examined, a condition known to trigger massive production of $^1O_2$ by PSII (Krieger-Liszkay and Trebst, 2006). Indeed, *mbs1-1* mutant plants showed severe symptoms of photooxidative damage under excess light (Figure 2C), consistent with an involvement of the *Arabidopsis* MBS1 protein in ROS responses. At the rosette stage, the phenotype was characterized by early senescence of the older leaves, indicative of the accumulation of light-induced oxidative damage over time.

In the absence of a second independent T-DNA mutant for *MBS1*, complementation of the *mbs1-1* mutant with an *MBS1-GFP* (for green fluorescent protein) fusion gene under the control of the native *MBS1* promoter was attempted. Transgenic lines (P_{MBS1}:*MBS1-GFP*/*mbs1-1* lines) were initially identified by their GFP fluorescence and subsequently assayed for complementation of the HL-sensitive *mbs1-1* phenotype. Four independently generated lines showed accumulation of the MBS1-GFP fusion protein and displayed wild-type-like tolerance to HL stress (Figures 2C; see Supplemental Figure 2 online), thus proving that the phenotype of the *mbs1-1* mutant is indeed caused by the T-DNA insertion and, at the same time, demonstrating that the MBS1-GFP fusion protein is functional.

In the absence of both a mutant for *MBS2* and a second independent T-DNA allele for *MBS1*, mutant lines for both genes were produced by RNA interference (RNAi). To this end, gene-specific tags were inserted into RNAi vectors and stably transformed into the *Arabidopsis* genome. For both *MBS1* and *MBS2*, RNAi lines could be isolated that showed varying amounts of gene-specific downregulation of expression at the mRNA level (Figure 2D). To generate a double mutant, the RNAi construct against *MBS2* was transformed into the *mbs1-1* mutant and homozygous *RNAi-MBS2 mbs1-1* mutants were isolated. They showed lack of detectable *MBS1* expression and low levels of *MBS2* expression (Figure 2D). While the phenotype of the *RNAi-MBS2* plants was similar to that of the *mbs1-1* mutant, the double mutants clearly showed a more severe phenotype in that premature leaf senescence occurred already at the early rosette stage (Figure 2E).

Accumulation of MBS Proteins in Stress Granules and mRNA Processing Bodies

To determine the subcellular localization of the MBS proteins in both *C. reinhardtii* and *Arabidopsis*, gene fusions to yellow fluorescent protein (*YFP*) (*C. reinhardtii*) and *GFP* (*Arabidopsis*) were constructed and introduced into cells by stable and transient transformation, respectively. Visualization of YFP fluorescence in *C. reinhardtii* was possible using the recently generated UV mutagenesis (UVM) expression strains (Karcher et al., 2009; Neupert et al., 2009). The MBS-YFP fusion protein showed a clear cytosolic localization in the transgenic algal strains (Figure 3A). Similarly, the *Arabidopsis* MBS1-GFP fusion protein accumulated in the nucleocytosolic compartment of transiently transformed tobacco (*Nicotiana tabacum*) protoplasts (Figure 3B). Interestingly, the localization pattern changed markedly when the cells were exposed to $^1O_2$ stress. The previously homogeneous distribution of the fluorescence in the cytosol was now confined to discrete spots (Figure 3C), raising the possibility that the perception of $^1O_2$ involves a pronounced change of MBS1 protein distribution in the cell.

Stress-related globular structures that are known to form in the cytosol include stress granules (SGs) and processing bodies (PBs). SGs accumulate under various stress conditions and represent large cytoplasmic aggregates of untranslated mRNAs bound to a specific set of proteins. As the mRNAs are stored in the form of stalled preinitiation complexes, translation initiation factors, such as RNA-binding protein47 (RBP47), can serve as molecular markers for SGs (Weber et al., 2008). PBs are stress-related cytoplasmic foci that contain enzymes involved in mRNA degradation. In plant cells, they can be distinguished from SGs using the DECAPPING1 (DCP1) subunit of the mRNA decapping complex as marker protein (Weber et al., 2008). To test for a possible association of MBS1 with SGs and/or PBs, constructs expressing fusions of the red fluorescent protein (RFP) to RBP47 or DCP1 (Weber et al., 2008) were employed in cotransformation experiments with the *MBS1-GFP* fusion construct. Interestingly, MBS1-GFP fluorescence showed clear overlap with both RFP-RBP47 and RFP-Dcp1 fluorescence, indicating that MBS1 associates with both SGs and PBs upon $^1O_2$ stress (Figure 3C; see Supplemental Figure 3 online). Light stress–dependent accumulation of MBS1 (and its concentration in cytoplasmic granular

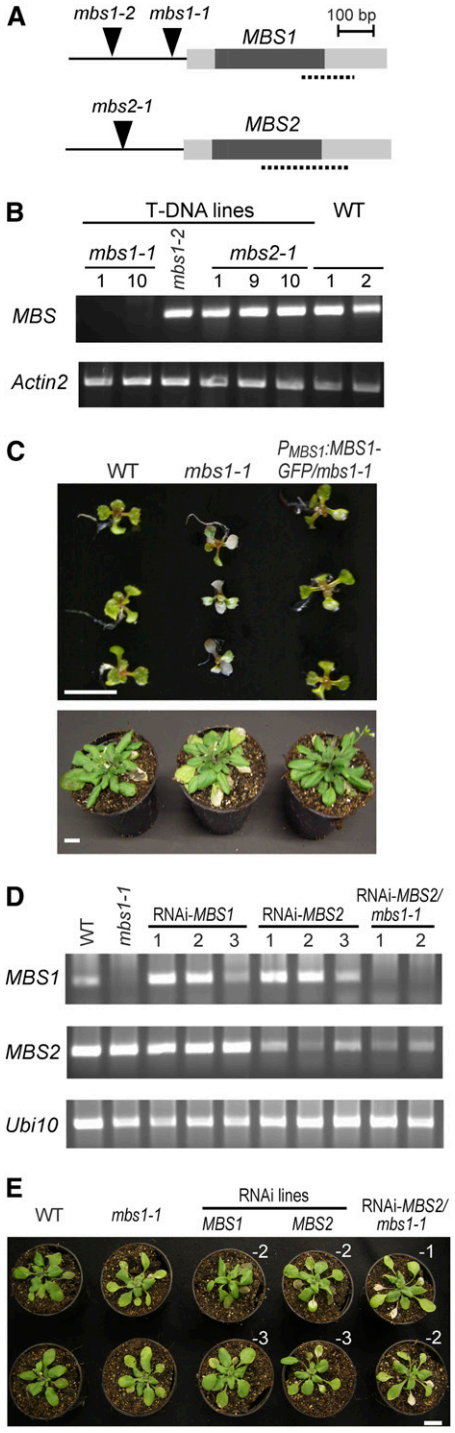

Figure 2. Characterization of *Arabidopsis MBS* Genes, Isolation of *mbs* Mutants, and Generation of RNAi Lines.

(A) Schematic structure of the *MBS1* and *MBS2* genes in *Arabidopsis* and identification of T-DNA insertion sites (arrowheads) in *mbs1* and *mbs2* mutant alleles. Dark boxes indicate coding regions, and gray boxes denote the 5′ and 3′ untranslated regions. The dotted lines indicate the gene-specific tags used for the construction of RNAi lines.

structures) was also seen in transgenic plants stably expressing the MBS1-GFP fusion protein (Figures 3D and 3E; see Supplemental Movie 1 online).

To ultimately confirm that MBS1 protein is associated with cytosolic RNA-containing granules, we enriched these granules from plants expressing the MBS1-GFP fusion protein using a protocol developed for PB purification (Teixeira et al., 2005). This procedure resulted in the isolation of fluorescent bodies that could be readily observed by confocal laser scanning microscopy (see Supplemental Figure 3B online). Treatment with RNase A resulted in loss of the granular GFP fluorescence suggesting that it dissolved the granules or at least released MBS1-GFP protein from the granules (see Supplemental Figure 3B online).

Light Stress Sensitivity and Accumulation of $^1O_2$ in *mbs* Mutants and Overexpression Lines

If *mbs* mutants are defective in $^1O_2$ sensing or signaling, they should be incapable of efficient induction of the antioxidative defense system that detoxifies $^1O_2$ after stress acclimation. To test for such defects, $^1O_2$ imaging of light-stressed *Arabidopsis* seedlings was performed by staining leaves with the $^1O_2$-specific fluorescent dye singlet oxygen sensor green (SOSG; Driever et al., 2009). Indeed, leaves of the *mbs1-1* mutant showed much more intense staining with SOSG than the wild type (Figure 4A), suggesting that the mutant is deficient in inducing $^1O_2$ detoxification reactions, presumable due to the lack of proper $^1O_2$ signaling. The effect was specific to $^1O_2$ in that staining for H_2O_2 accumulation with diamino benzidine revealed no significant difference between the wild type and the mutant (see Supplemental Figure 4 online).

To study the effects of *MBS1* overexpression, an additional set of transgenic lines was generated (in addition to the complemented P_{MBS1}*:MBS1-GFP/mbs1-1* lines; see above), in which

(B) Expression analysis of *MBS1* and *MBS2* in T-DNA insertion mutants. RT-PCR analysis demonstrates the absence of *MBS1* transcripts from the *mbs1-1* T-DNA line (1 and 10 indicate two different homozygous plants isolated), whereas *MBS1* transcripts are detectable in the homozygous *mbs1-2* line and *MBS2* transcripts are detectable in the *mbs2-1* plants. *Actin2* was used as an internal control. WT, wild type.

(C) Sensitivity of *mbs1-1* mutant plants to HL stress. Twelve-day-old seedlings grown on synthetic medium were exposed to 900 μE m^{-2} s^{-1} for 2 d (top panel), and 4-week-old plants grown in soil were exposed to 1000 μE m^{-2} s^{-1} for 3 d and then transferred back to 600 μE m^{-2} s^{-1} for 4 d (bottom panel; cf. Supplemental Figure 2 online). The wild type, the *mbs1-1* mutant, and the complemented line P_{MBS1}*:MBS1-GFP/mbs1-1* were analyzed (for three additional independently generated complemented lines, see Supplemental Figure 2 online). Bars = 1 cm.

(D) RT-PCR analysis of *MBS1* and *MBS2* mRNA accumulation in the wild type, *RNAi-MBS1* lines, *RNAi-MBS2* lines, and *RNAi-MBS2 mbs1-1* double mutant lines. The *Ubi10* mRNA served as internal control.

(E) Increased sensitivity of the *RNAi-MBS2 mbs1-1* double mutant to HL stress compared with the *mbs1-1* single mutant and the RNAi lines against *MBS1* and *MBS2*. Plants were exposed to 1000 μE m^{-2} s^{-1} for 3 d and then transferred back to 600 μE m^{-2} s^{-1} for 2 d. Independently generated lines are indicated by white Roman numerals. Bar = 1 cm.

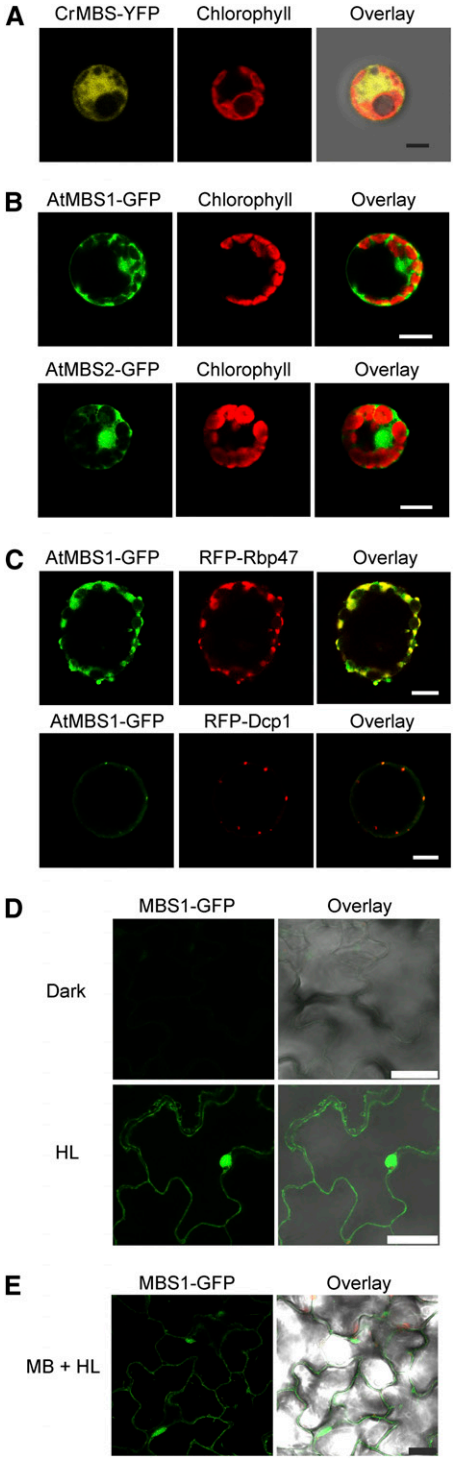

Figure 3. Subcellular Localization of MBS1 under Normal Conditions and under $^1O_2$ Stress.

(A) Localization of a Cr-MBS-YFP fusion protein in stably transformed *C. reinhardtii* cells. MBS is localized in the cytosol and the nucleus. YFP fluorescence, chlorophyll fluorescence, and the overlay of YFP fluorescence, chlorophyll fluorescence, and the bright-field image are shown. Bar = 3 μm.

the *MBS1* transgene is driven by the strong constitutive cauliflower mosaic virus (CaMV) 35S promoter in the *msb1-1* mutant background (*35S:MBS1/mbs1-1* lines). As expected, these lines also showed complementation of the *mbs1-1* mutant phenotype, including full restoration of $^1O_2$ signaling and detoxification reactions in response to light stress (Figure 4A).

SOSG staining was also employed to investigate $^1O_2$ accumulation at the subcellular level. As a control, the *Arabidopsis flu* mutant was included, which accumulates the photosensitizer protochlorophyllide in the dark and, after a dark-to-light shift, generates massive amounts of $^1O_2$ in the chloroplast (op den Camp et al., 2003; Wagner et al., 2004). As expected, this was seen as intense SOSG fluorescence upon transfer of mutant plants to the light (Figure 4B). By contrast, wild-type plants did not show significant changes in SOSG fluorescence even upon transfer to HL, presumably because of the efficient induction of $^1O_2$ signaling mechanisms and detoxification reactions. The *mbs1-1* mutant, however, showed strong accumulation of $^1O_2$ in chloroplasts in response to light stress (Figure 4B), confirming that the chloroplast is the main site of $^1O_2$ production also in the *mbs1-1* mutant and providing further evidence for this mutant not properly responding to $^1O_2$.

Extensive work on the *flu* mutant has shown that, under low-level photooxidative stress, $^1O_2$ production does not directly cause lethal cellular damage, but instead, activates a genetic program (dependent on the function of the EXECUTER1 protein) that ultimately results in cell death, seedling lethality, and inhibited plant growth (Wagner et al., 2004). At higher levels of photooxidative stress, this genetically controlled response is gradually overridden by the physiological cell death response triggered by $^1O_2$ toxicity. When the sensitivity of the *mbs1-1* mutant to photooxidative stress was analyzed in dark-light shift experiments, it was found to be highly sensitive (with ~80% seedling lethality), albeit significantly less sensitive than the *flu* mutant (that showed 100% lethality; Figure 4C).

(B) Localization of At-MBS1-GFP and At-MBS2-GFP fusion proteins in transiently transformed tobacco protoplasts. Both proteins are localized in the cytoplasm and the nucleus under nonstressed conditions. Images were obtained 48 h after protoplast transformation. Bars = 10 μm.

(C) At-MBS1 localizes to cytoplasmic SGs and PBs under $^1O_2$ stress. AtMBS1-GFP was transiently coexpressed in tobacco protoplasts with either the SG marker Rbp47 or the PB marker Dcp1 (Weber et al., 2008). Colocalization in cytoplasmic foci was observed 30 min after induction of $^1O_2$ stress by exposure to HL (500 μE m^{-2} s^{-1}) in the presence of 1 μM MB. Note that PBs are much smaller than SGs, which is an observation that was consistently made in all protoplasts showing PB staining (cf. Supplemental Figure 3 online). The smaller size of the PBs correlates with lower levels of MBS1-GFP accumulation, possibly due to reduced stability of the protein molecules that are not incorporated into PBs. Bars = 10 μm.

(D) MBS1-associated cytoplasmic foci induced in cells of the upper epidermis by HL treatment (1000 μE m^{-2} s^{-1}) for 3 h after 2 d of preincubation in the dark. The assays were performed with *Arabidopsis* seedlings that stably express the P_{MBS1}*:MBS1-GFP* fusion gene in the *mbs1-1* mutant background. Bars = 25 μm.

(E) Image from a movie of MBS1-associated cytoplasmic foci trafficking under $^1O_2$ stress in P_{MBS1}*:MBS1-GFP/mbs1-1* seedlings (cf. Supplemental Movie 1 online). Bar = 25 μm.

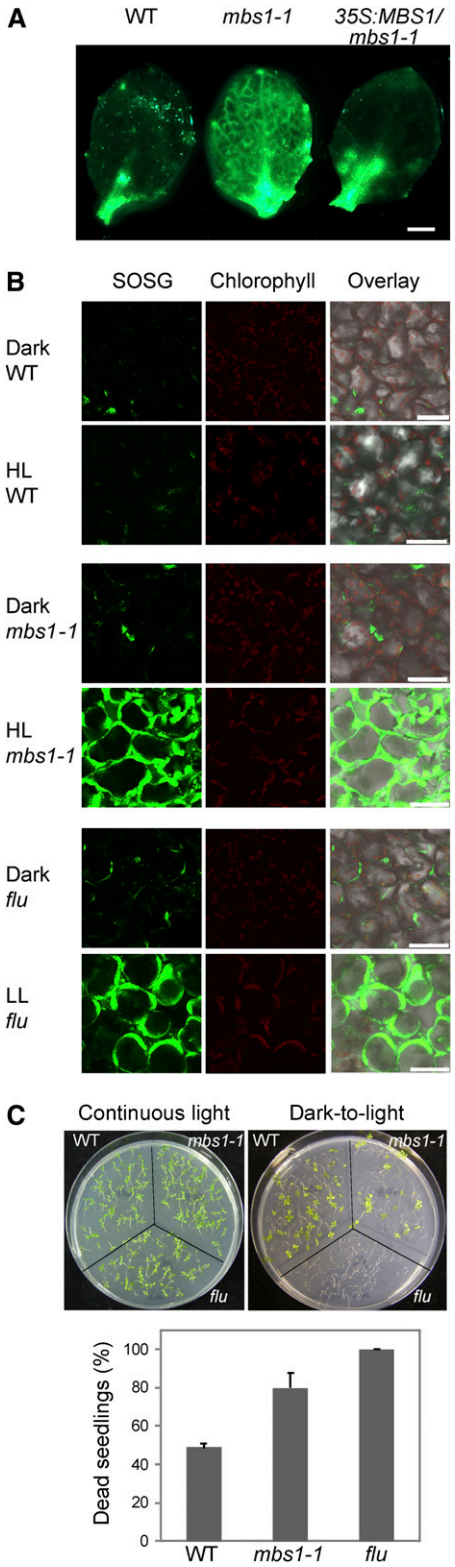

Figure 4. $^1O_2$ Accumulation in the *Arabidopsis mbs1-1* Mutant under Light Stress.

Light sensitivity of the *mbs1-1* mutant was further confirmed by measurements of the maximum quantum efficiency of PSII, F_v/F_m. Upon HL stress, F_v/F_m declined sharply in the mutant compared with the wild type (see Supplemental Figure 5 online), suggestive of the accumulation of photooxidative damage in PSII. Altogether, these data are consistent with an important role of the MBS protein in triggering appropriate cellular responses to $^1O_2$ stress.

Expression of ROS-Responsive Marker Genes in *mbs* Mutant Plants

Taken together, the data on the *C. reinhardtii* and *Arabidopsis* mutants establish that *mbs* mutants produce $^1O_2$ upon photooxidative stress, but cannot properly induce cellular defense responses. In *C. reinhardtii*, this is also evident at the level of $^1O_2$-responsive gene expression (Figure 1). To test whether the *Arabidopsis mbs1-1* mutant is defective in ROS-responsive gene expression, quantitative real-time RT-PCR (qRT-PCR) assays were performed for marker genes of oxidative stress (Figure 5). The *Arabidopsis flu* mutant was included as a control because it shows extreme induction of $^1O_2$-responsive gene expression, due to the massive production of $^1O_2$ after transition from darkness (or low light) to HL conditions (op den Camp et al., 2003; Wagner et al., 2004). Analysis of *MBS1* expression in the wild type and the *flu* mutant revealed that *MBS1* itself is not inducible at the mRNA level by $^1O_2$ stress (Figure 5). qRT-PCR using specific primers for the $^1O_2$ marker genes *AAA* (for AAA-ATPase; Baruah et al., 2009), *BAP1* (for *BON ASSOCIATION PROTEIN1*; Baruah et al., 2009), and *Toll-IR* (for Toll-Interleukin-Resistance domain-containing protein; Ramel et al., 2012a) revealed rapid induction of expression in the *flu* mutant already 1 h after the shift to HL stress (which slightly decreased after 3 h) and moderate induction in the wild type after 1 h (followed by a decline after 2 h and another increase after 3 h). By contrast, no increase above the level at time point zero was seen in the expression of any of the three $^1O_2$ marker genes in the *mbs1-1* mutant (and overall, the expression levels tended to even decrease).

To test whether or not other ROS responses are also impaired in the *mbs1-1* mutant, the expression of two H_2O_2 marker genes

(A) $^1O_2$ imaging of light-stressed *Arabidopsis* seedlings by staining of leaves with SOSG. Leaves of the wild type (WT), the *mbs1-1* mutant, and the *35S:MBS1/mbs1-1* transgenic line were analyzed. For quantitation of SOSG fluorescence, see Supplemental Figure 9 online. Bar = 1 mm.

(B) Accumulation of $^1O_2$ in chloroplasts of mesophyll cells in the wild type, the *mbs1-1* mutant, and the *flu* mutant of *Arabidopsis* in response to light stress. Cells were stained with SOSG, and fluorescence was detected by confocal laser scanning microscopy. As a control, the *flu* mutant, which generates $^1O_2$ upon transition from dark to light (op den Camp et al., 2003), was exposed to low light (LL). Bars = 50 μm.

(C) Light induction of the cell death response in seedlings of the *mbs1-1* mutant and the *flu* mutant. Seedlings were either grown in continuous light (top left panel) or kept in the dark for 5 d followed by transfer to the light (8-h-dark/16-h-light diurnal cycle; top right panel) to trigger $^1O_2$ production. The graph (bottom panel) shows the death rates of seedlings as scored in three independent dark-to-light shift experiments. Values represent means ± SD.

was analyzed: *ASCORBATE PEROXIDASE1* (*APX1*; Baruah et al., 2009) and *CATALASE2* (*CAT2*; Du et al., 2008). Both genes showed similar induction behavior upon light stress in the wild type, the *flu* mutant, and the *mbs1-1* mutant (Figure 5), indicating that the responses to H_2O_2 are largely unaffected. Finally, two general light stress–responsive transcription factors were investigated: *ZAT12* (Baruah et al., 2009) and *WRKY40* (Adhikari et al., 2011). Their induction by light stress was delayed or less pronounced in the *mbs1-1* mutant compared with the wild type and the *flu* mutant, possibly due to the lack of the contribution of the $^1O_2$ signal to the induction. Together, these data suggest that, at the level of gene expression, the *mbs1-1* mutant does not respond properly to $^1O_2$, while it shows largely unaffected responses to other ROS.

MBS1 Overexpression Leads to Enhanced Tolerance to Photooxidative Stress

Using the *35S*:*MBS1* construct (see above), transgenic *Arabidopsis* lines overexpressing the MBS1 protein were generated. Nonquantitative RT-PCR analyses indicated that, at the mRNA level, substantial overexpression of the *MBS1* gene could be achieved (Figure 6A). To be able to assess expression at the protein level, specific antibodies against the MBS1 protein were generated. The antibodies recognized the MBS1 protein with high specificity but were not sensitive enough to detect the protein in wild-type plants, possibly suggesting that the expression level is low or protein detection is difficult due to the small size of MBS1 (of only 11.3 kD). However, in two MBS1 overexpression lines (*35S*:*MBS1*-8 and *35S*:*MBS1*-28; Figure 6B), the antibodies detected the MBS1 protein, demonstrating that strong overexpression was achieved also at the protein level. The MBS1 overexpression lines were visually indistinguishable from wild-type plants and *mbs1-1* mutant plants under normal light conditions (120 μE m^{-2} s^{-1}). However, when exposed to HL stress (at 1000 μE m^{-2} s^{-1}; Figure 6C), the MBS1 overexpression lines showed a much stronger accumulation of the stress-protective pigment anthocyanin than the wild type, while the *mbs1-1* mutant (and also the *RNAi-MBS2 mbs1-1* mutant) showed a pale phenotype and lacked visible accumulation of anthocyanin (although some low-level induction of anthocyanin biosynthesis was measurable; Figures 6C and 6D). It is well established that anthocyanin synthesis is induced upon exposure to HL (and other types of oxidative stress), but this induction is largely inhibited by overaccumulation of ROS (Vanderauwera et al., 2005). Thus, the pattern of anthocyanin accumulation in the *mbs* mutants and overexpression lines confirms that $^1O_2$ overaccumulation occurs in the *mbs* mutants and suggests that light stress responses are induced more efficiently in the MBS1 overexpression lines. The stronger protective response to HL stress translates into a pronounced growth advantage of the MBS1 overexpression lines after transfer back to normal light conditions (Figure 6C). High tolerance of the overexpression lines to light stress (and hypersensitivity of the *mbs* mutants) was further confirmed by measurements of the change in chlorophyll content (which declined less severely in the overexpression lines than in the wild type) and in the maximum quantum efficiency of PSII (which did not decline in the wild type and the overexpression lines) during the recovery from HL stress (Figure 6D).

The anti-MBS1 antibody also detected the MBS1-GFP protein in one of our complemented lines that were transformed with the *MBS1-GFP* construct under the control of the endogenous *MBS1* promoter (Figure 6B). This allowed us to determine MBS1 protein accumulation in response to HL stress. Indeed, the protein accumulated to elevated level after transfer from normal light to HL (Figure 6B). As light stress does not significantly alter *MBS1* mRNA levels (Figure 5), this finding suggests that MBS1 accumulation is regulated at the translational or posttranslational level. Light stress–induced MBS1-GFP accumulation also explains the strong increase in GFP fluorescence after transfer from the dark to HL conditions observed in our subcellular localization analyses (Figure 3D).

Assuming that MBS proteins act as components of $^1O_2$ signaling, but do not function as a scavenger of $^1O_2$, MBS-expressing bacterial strains should not show an elevated tolerance to $^1O_2$ stress, as the MBS-overexpressing plants do. To confirm this, the *MBS* genes from *C. reinhardtii* (Cr-*MBS*) and *Arabidopsis* (At-*MBS1*) were expressed under the control of an isopropyl–β–D–thiogalactopyranosid–inducible promoter in *Escherichia coli.* When the strains were challenged with $^1O_2$ stress induced by MB treatment, no increased tolerance was seen in the stains overexpressing Cr-MBS or At-MBS1 (see Supplemental Figure 6 online), suggesting that the MBS protein does not act as a $^1O_2$ scavenger.

Global Analysis of ROS-Responsive Gene Expression in *mbs* Mutants and Overexpression Plants

Transcriptome profiling experiments were performed for the following five lines: *mbs1-1*, *RNAi-MBS2 mbs1-1*, *35S*:*MBS1*, *flu*, and the wild type. Plants were stressed by shifting them from a 3-h dark period to HL for 3 h and compared with unstressed control plants at the end of the 3-h dark period (see Methods) in three biological replicates using Affymetrix ATH1 microarrays. When the numbers of genes in the genome that displayed a more than fourfold significant change 3 h after the onset of light stress (P value threshold set to 0.05 based on Student's *t* test with false discovery rate correction) were compared, the *flu* mutant showed the strongest change (Figure 7A). The number of induced genes was elevated compared with the wild type and the other plant lines investigated, consistent with the *flu* mutant suffering from severe photooxidative stress upon transfer from low light to light stress conditions.

To assess the regulation of ROS-responsive genes, we extracted from the microarray data sets all *Arabidopsis* genes that had been reported as specifically responding to $^1O_2$ or H_2O_2/O_2^- based on previously performed comprehensive transcriptomic studies using the same microarrays (Affymetrix ATH1; op den Camp et al., 2003; Gadjev et al., 2006). This gave a set of 625 $^1O_2$-responsive genes (=617 probe sets on the ATH1 array) and 638 H_2O_2/O_2^--responsive genes (=597 probe sets; see Supplemental Data Set 1 online). These sets were then analyzed in the five plant lines (Figure 7; see Supplemental Figures 7 and 8 and Supplemental Data Set 2 online). As expected, the ROS-responsive gene expression pattern in the *flu* mutant differed most strongly from that of

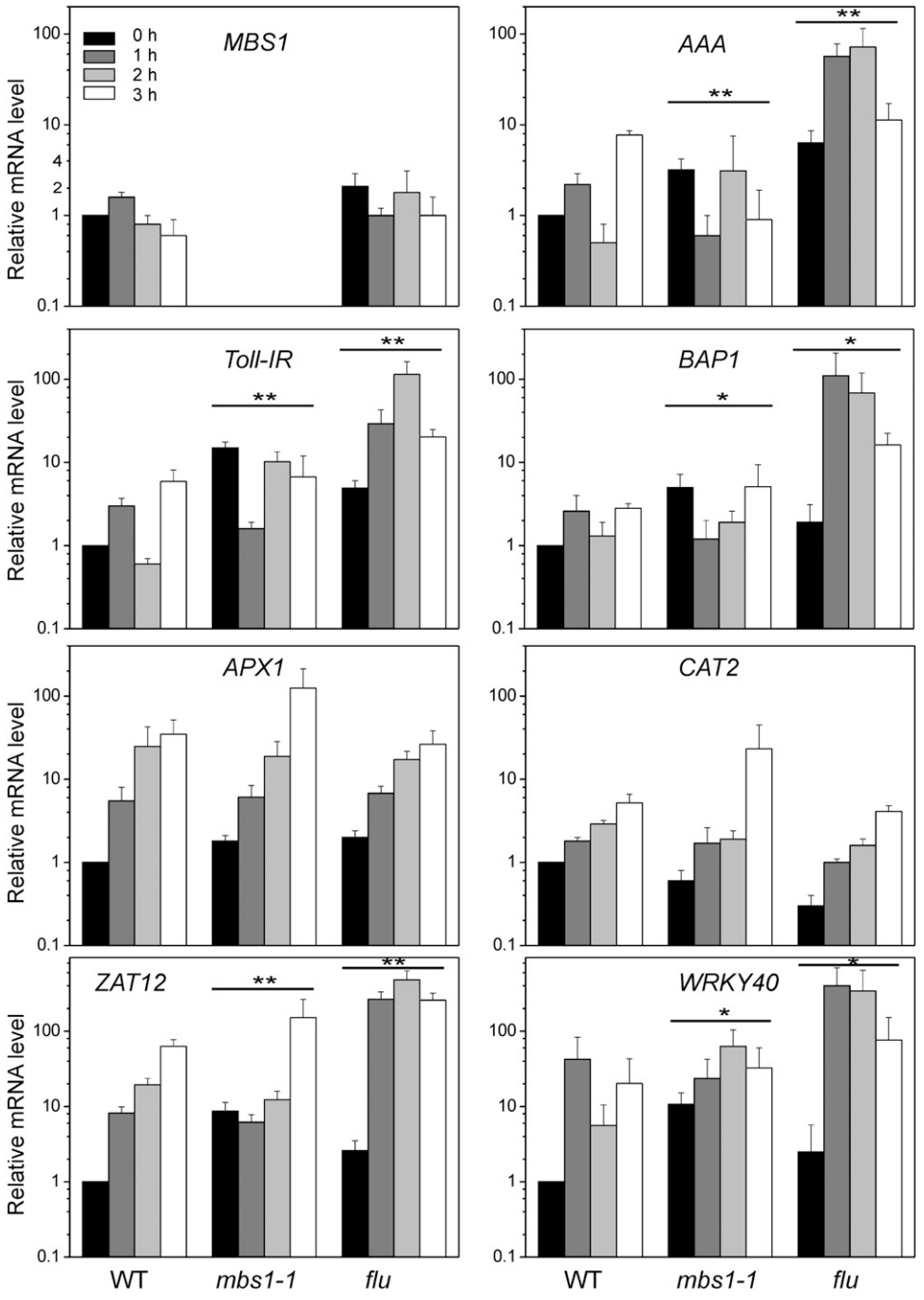

Figure 5. Deregulation of $^1O_2$-Inducible Genes in the *mbs1-1* Mutant under Light Stress.

Expression of marker genes of oxidative stress responses in *mbs1-1* is compared with the wild type (WT) and the *flu* mutant. The expression levels of ROS-responsive genes were measured over four time points by qRT-PCR using specific primers for the $^1O_2$ marker genes *AAA* (At3g28580), *BAP1* (At3g61190), and *Toll-IR* (At3g50970), the H_2O_2 marker genes *APX1* (At1g07890) and *CAT2* (At4g35090), and the two ROS-responsive transcription factors *ZAT12* (At5g59820) and WRKY40 (At1g80840). mRNA levels were determined by the $2^{-\Delta\Delta CT}$ method relative to the wild-type sample at time point 0 h, which was assigned a value of 1. Data are mean values ± SD of three biological replicates. Statistical analysis of the data was performed by two-way analysis of variance. Differences between expression patterns in the mutants and the wild type that are significant at the level of $^{**}P \leq 0.001$ or $^{*}P \leq 0.01$.

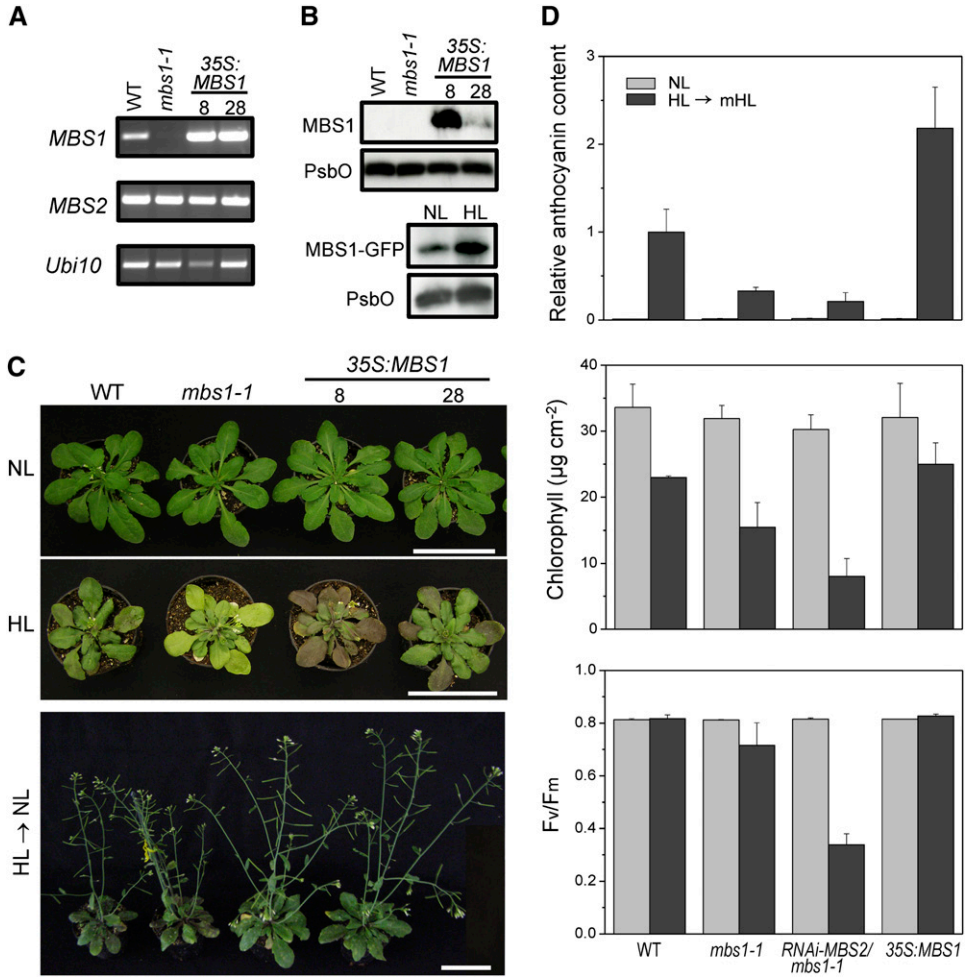

Figure 6. *MBS1* Expression Levels Determine the HL Tolerance of Plants.

(A) *MBS* transcript levels in the wild type (WT), the *mbs1-1* mutant, and two *MBS1* overexpression lines (8 and 28). RT-PCR analysis demonstrates overexpression of *MBS1* in the *35S*:*MBS1* transgenic lines. *MBS2* and *Ubi10* served as internal controls.

(B) MBS1 protein levels in the wild type, the *mbs1-1* mutant, and the *MBS1*-overexpressing lines. While in the wild type, the 11.3-kD MBS1 protein is not expressed to levels detectable with the sensitivity of our anti-MBS1 antibody, the protein is readily detected in the *35S*:*MBS1* overexpression lines (top panel). The protein is also detectable in one of the complemented lines expressing MBS1-GFP from the endogenous *MBS1* promoter (bottom panel). To measure expression in response to HL stress, 4-week-old P_{MBS1}:*MBS1-GFP* plants grown in soil were treated with HL (1000 μE m^{-2} s^{-1}) for 3 h and then transferred to normal light (NL; 120 μE m^{-2} s^{-1}) for 45 min. Untreated plants were maintained in normal light (120 μE m^{-2} s^{-1}). Fifteen micrograms of total protein per sample was loaded. The PSII protein PsbO was used as loading control.

(C) Comparison of the phenotypes of wild-type plants, the *mbs1-1* mutant, and two *35S*:*MBS1* overexpression lines under normal light conditions (μE m^{-2} s^{-1}; 5-week-old plants; top panel), under HL stress (4-week-old plants exposed to light stress at 1000 μE m^{-2} s^{-1} for 5 d in a 16-h-HL/8-h-dark cycle; middle panel), and after recovery from HL and continued growth for 21 d under normal light (HL → NL; bottom panel). Bars = 6 cm.

(D) Light stress acclimation in *Arabidopsis MBS* mutants and overexpression plants. Anthocyanin contents, chlorophyll contents, and PSII activities were compared under light stress conditions (HL → mHL; 1000 μE m^{-2} s^{-1} for 3 d and then transfer to 600 μE m^{-2} s^{-1} for 3 d; 16-h-light/8-h-dark regime) and normal light (120 μE m^{-2} s^{-1}). The wild type, the *mbs1-1* and RNAi-*MBS2 mbs1-1* mutants, and a transgenic *35S*:*MBS1* overexpression line were analyzed. Anthocyanin contents are displayed as relative values to the wild type after the stress treatment, which was assigned a value of 1. Data represent mean values ± SD of three biological replicates.

the other four lines. The wild type grouped together with the *35S*:*MBS1* overexpression line, and the two *mbs* mutant lines (*mbs1-1* and *RNAi-MBS2 mbs1-1*) clustered together. Interestingly, in the mutant lines, the number of $^1O_2$ marker genes significantly induced by more than fourfold by HL stress was much lower than in the wild type (Figure 7B). Whereas 51 $^1O_2$-responsive genes were upregulated in the wild type, only 16 were upregulated in the *RNAi-MBS2 mbs1-1* double mutant (Figure 7B), supporting the idea that the MBS gene product is required to mediate $^1O_2$ responses at the level of gene expression. By contrast, the number of H_2O_2/O_2^--responsive genes induced in the mutants was only slightly lower than in the wild type and the *35S*:*MBS1*

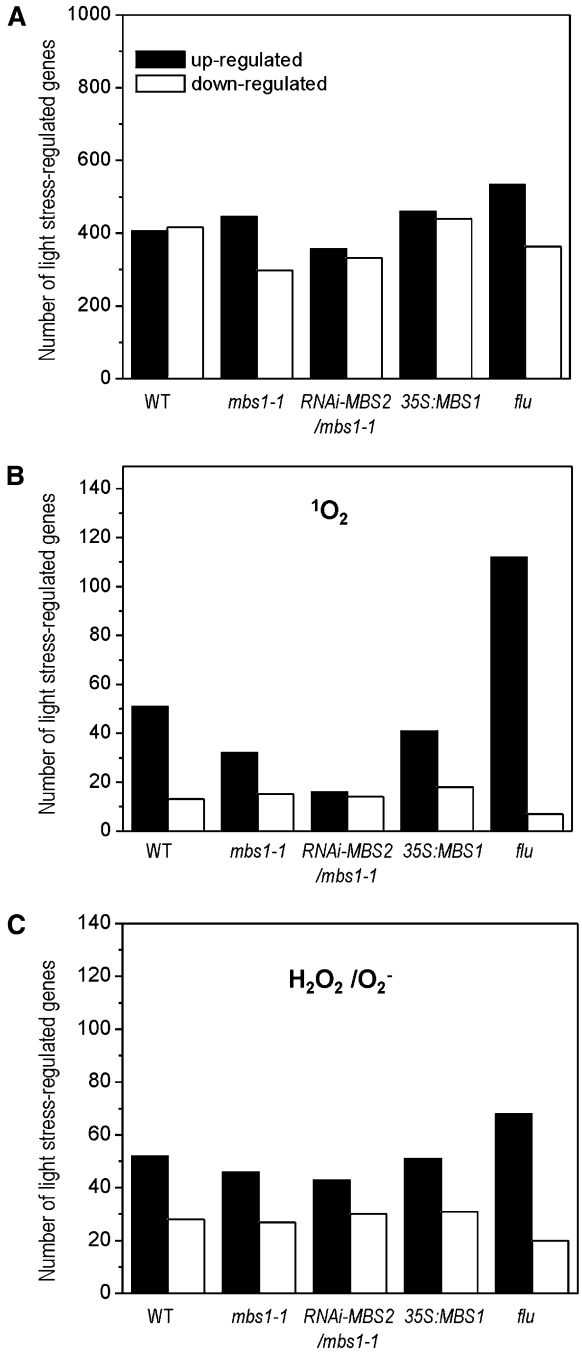

Figure 7. Light Stress–Responsive Gene Expression in the Wild Type, the *mbs1-1* Mutant, the *RNAi-MBS2 mbs1-1* Double Mutant, the *35S:MBS1* Overexpression Line and the *flu* Mutant.

The genome-wide response of the transcriptome to a sudden shift from low-light to HL conditions was determined by microarray analysis.

(A) Light stress response of all genes represented on the ATH1 arrays. Total numbers of genes in the five plant lines that displayed a significant and greater than fourfold change 3 h after the onset of light stress. WT, wild type.

(B) Light stress response of the subset of genes previously reported as responsive to $^1O_2$ (op den Camp et al., 2003; Gadjev et al., 2006). Panel shows number of genes in the subset showing significant and greater than fourfold response in the microarray analysis (see Supplemental Data Set 2 online).

(C) Light stress response of the subset of genes previously reported as responsive to H_2O_2/O_2^- (Gadjev et al., 2006). Panel shows number of genes in the subset showing significant and greater than fourfold response in the microarray analysis (see Supplemental Data Set 2 online).

line, suggesting that these responses are not primarily affected in the *mbs* mutants (Figure 7C).

MBS accumulates in the nucleocytosolic compartment. $^1O_2$ is mainly produced in the chloroplast as a by-product of photosynthetic electron transfer (Apel and Hirt, 2004). The chloroplast is also an important site where $^1O_2$-mediated adaptation responses occur to scavenge $^1O_2$ and minimize its production. The latter includes a transcriptional response of the chloroplast genome (Coll et al., 2009), which encodes many of the key components of the ROS-producing photosystems, especially the reaction center subunits of both photosystems which bind a large number of redox-active cofactors. Chloroplast photosynthesis genes are mainly transcribed by the plastid-encoded RNA polymerase, which resembles bacterial RNA polymerases and requires nuclear-encoded sigma factors for promoter recognition (Liere and Börner, 2007). Sigma factors, in turn, are regulated by sigma factor binding proteins (Lai et al., 2011). In *Arabidopsis*, the SIGMA FACTOR BINDING PROTEIN1 (SIB1) is rapidly induced by $^1O_2$ stress (op den Camp et al., 2003) and by pathogen attack (Lai et al., 2011), the response to which also involves ROS production and extensive ROS-mediated signal transduction (Lam et al., 2001; Apel and Hirt, 2004). Our microarray experiments indicated that the transcriptional induction of the *SIB1* gene in response to HL stress is abrogated in *mbs* mutants (see Supplemental Data Sets 1 and 2 online). In view of the key role that SIB1 and plastid sigma factors play in mediating primary stress responses in chloroplast gene expression (Coll et al., 2009; Lai et al., 2011), we sought to confirm this finding using an independent method. qRT-PCR analyses demonstrated that neither the *mbs1-1* mutant nor the *RNAi-MBS2 mbs1-1* mutant were capable of inducing the expression of the *SIB1* gene in response to HL stress, whereas the *35S:MBS1* overexpression line showed a wild-type-like response (Figure 8). These data provide further evidence for *mbs* mutants being impaired in their response to $^1O_2$ at the level of nuclear gene expression and, moreover, suggest that also the $^1O_2$-induced remodeling of chloroplast gene expression is defective in the mutants.

DISCUSSION

In this work, we used the model alga *C. reinhardtii* to isolate new components of ROS signaling in plants, employing a genetic screen based on the versatile reporter luciferase. This was made possible by the development of a new luciferase reporter (Shao and Bock, 2008) that, in spite of the often low transgene expression levels in *C. reinhardtii*, is sensitive enough to allow the identification of mutants that are defective in their capacity to induce reporter gene expression in response to an environmental stimulus.

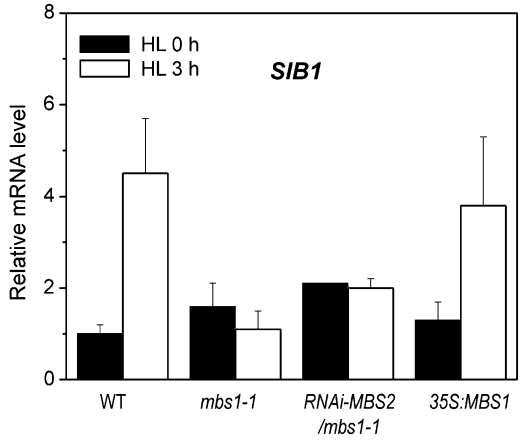

Figure 8. *MBS1* Inactivation Affects the Light Stress Response of the Chloroplast-Localized SIB1.

Expression of *SIB1* (At3g56710) was measured by qRT-PCR analysis in *Arabidopsis* wild-type plants (WT), the *mbs1-1* mutant, the *RNAi-MBS2 mbs1-1* mutant, and the *35S:MBS1* overexpression line. Twelve-day-old seedlings incubated under continuous light of 10 μE m^{-2} s^{-1} for 7 d on agar plates were exposed to HL stress (1000 μE m^{-2} s^{-1}). Samples were collected prior to the onset of light stress (HL 0 h) and 3 h after transfer to HL (HL 3 h). The relative mRNA levels of *SIB1* were quantified relative to the expression level in the wild type at 0 h, to which a value of 1 was assigned. Data are mean values ± SD of three biological replicates.

For the genetic dissection of ROS signaling pathways, the green alga *C. reinhardtii* offers significant advantages over higher plants, most of which are related to its unicellularity. Multicellular eukaryotes sense stresses and respond to them by a highly complex network of tissue-specific, cell-specific, and developmentally regulated pathways. For example, while abscisic acid is often regarded as a general stress hormone in plants that mediates responses to nearly all types of abiotic stresses, its biosynthesis is largely confined to specific tissues and cell types, and dedicated trafficking pathways are required to transport the hormone from its site of synthesis to its sites of action (Galvez-Valdivieso et al., 2009; Antoni et al., 2011; Seo and Koshiba, 2011). By contrast, stress perception and stress responses in *C. reinhardtii* all occur in a single cell. An additional advantage of the alga's unicellularity relates to the application of inhibitors or ROS-generating chemicals in genetic screens. Uptake of these compounds is much more homogeneous in a single-celled alga (compared with application by spraying or watering in a higher plant); consequently, the intracellular concentrations of these chemicals can be controlled precisely. This helps to avoid toxic effects from local overconcentration as well as problems with limited efficacy due to inefficient distribution within the plant. In view of the complexity of ROS signaling in multicellular eukaryotes (Gill and Tuteja, 2010; Møller and Sweetlove, 2010; Finkel, 2011; Mittler et al., 2011) and the need to keep the intracellular ROS concentrations tightly controlled to prevent initiation of cell death programs, genetic screens based on sensitive reporter genes in *C. reinhardtii* offer a powerful tool for the identification of new components of ROS sensing and signaling pathways. In this study, we demonstrated the validity of this approach by isolating a new component of $^1O_2$ signaling. By characterizing the homologous genes in the model plant *Arabidopsis*, we have also shown that new knowledge acquired about ROS signaling in *C. reinhardtii* is directly transferable to higher plants.

The *mbs* mutants isolated in the course of this study are unique in that they produce $^1O_2$ in response to photosensitizer treatment or HL stress but are unable to induce the appropriate cellular responses that ultimately help the organism to cope with the oxidative stress by inducing defense and detoxification mechanisms. The *mbs* mutants are blocked early in their $^1O_2$ responses, as evident by the failure to induce expression of $^1O_2$-responsive genes. Compared with the *C. reinhardtii mbs* mutant, $^1O_2$-responsive gene expression is not completely abrogated in the *Arabidopsis mbs1-1* mutant (cf. Figures 1 and 5), presumably due to the presence of a second homolog encoded by the *MBS2* locus. Interestingly, genes encoding ROS-responsive transcription factors show much more pronounced changes over time in the *flu* mutant than in the *mbs1-1* mutant, consistent with $^1O_2$ overproduction in *flu* (op den Camp et al., 2003) and an MBS1 action early in $^1O_2$ sensing or signaling, upstream of the induction of gene expression programs. Whether the MBS protein acts directly as a $^1O_2$ sensor or rather as an early component in $^1O_2$ signal transduction remains to be clarified. The single conserved zinc finger in the MBS proteins (Figure 1G) could confer a sensor-like property, in that it theoretically could react with $^1O_2$ and, for example, trigger a conformational response. However, thorough in vitro studies with the purified MBS protein will be required to substantiate this hypothesis. Our observation that MBS1 associates with RNA granules (SG and PBs; Figure 3) in a stress-dependent manner suggests that it might control the stability and/or translation of a specific set of mRNAs encoding signaling components and/or antioxidative defense components downstream of MBS1.

$^1O_2$ is generally known to be short-lived. In conjunction with photosynthetic electron transfer being its major source of production, the short half-life of $^1O_2$ has cast some doubt on its potential to leave the chloroplast and activate signaling pathways in the cytosol and/or the nucleus. However, based on the lifetime of $^1O_2$ measured in animal cells (of ~3 μs), it has been calculated that 5 to 10% of the $^1O_2$ produced in the chloroplast should be able to diffuse over the average distance between the chloroplast and the nucleus in *C. reinhardtii* cells (Fischer et al., 2007, and references therein). Interestingly, photooxidative stress–induced gene expression profiles of the *flu* mutant (producing $^1O_2$ in the stroma) and the *ch1* mutant (producing $^1O_2$ at PSII in the thylakoid membrane) are very similar (Ramel et al., 2013b), providing further support of the idea that $^1O_2$ can diffuse at least over some distance. In this context, it is important to note that the possibility of $^1O_2$ directly acting as a signaling molecule and the recently established signaling function of molecules derived from chemical reactions with $^1O_2$ (such as the carotenoid oxidation product β-cyclocitral; Ramel et al., 2012a, 2012b) are not mutually exclusive, not the least because multiple $^1O_2$-dependent signaling pathways are likely to coexist in plants (Lee et al., 2007; Kim et al., 2012; Ramel et al., 2013a).

An *Arabidopsis mbs1/mbs2* double knockout is currently not available, and, due to the small size of the *MBS* genes, isolation of a T-DNA insertion line for *MBS2* may be difficult to achieve.

However, together with the high sequence similarity at the protein level and the presence of only one *MBS* gene in the genomes of *C. reinhardtii* and rice (Figure 1G), the aggravated phenotype of our *RNAi-MBS2 mbs1-1* double mutants (Figure 2) strongly suggests that the two *Arabidopsis MBS* genes serve overlapping if not redundant functions. The genomic regions in which *MBS1* and *MBS2* are embedded on chromosome 3 and chromosome 5, respectively, contain several other duplicated genes, suggesting duplication of a larger chromosomal segment as the likely origin of the two *MBS* genes in *Arabidopsis*. Whether or not *MBS* gene retention in the duplicated region is the result of selection (i.e., reflects an adaptation to stressful environments) remains to be investigated. Interestingly, our overexpression analyses clearly indicate that the amount of MBS1 protein is positively correlated with tolerance to photooxidative stress (Figure 6), further supporting an important role of MBS1 in ROS signaling. Our results also suggest overexpression of *MBS* genes as a suitable strategy to improve the stress tolerance of crop plants.

Given the multifarious roles that ROS play in physiological and developmental processes (Jiang et al., 2012) as well as in abiotic stress signaling (Jaspers and Kangasjärvi, 2010), retrograde signaling (Pogson et al., 2008), and cell death programs (Lam, 2008), a better knowledge of the cellular processes controlling ROS production and homeostasis and a deeper understanding of the underlying signaling and response pathways are of utmost importance. The combination of sensitive genetic screens in *C. reinhardtii* with subsequent functional analyses in both algae and higher plants provides a powerful strategy to dissect ROS responses and identify new players in the cellular networks controlling ROS homeostasis, sensing, and signaling. The identification of MBS1 provides proof of principle for this approach, and the many other mutants isolated in our genetic screen will provide a rich source for future investigations into the mechanisms of $^1O_2$ signaling.

METHODS

Algal Strains and Culture Conditions

Mutant screening was performed in a transgenic algal strain derived from *Chlamydomonas reinhardtii* strain 325 (CW15, *mt+*, *arg7-8*). The reporter gene cassette consisting of the codon-optimized luciferase gene from *Gaussia princeps* and the $^1O_2$-inducible *HSP70A* promoter was described previously (Shao and Bock, 2008). Subcellular localization analyses were performed in the *C. reinhardtii* expression strain UVM11 (Neupert et al., 2009). Algal cultures were grown photoheterotrophically in Tris-acetate phosphate (TAP) medium (Harris, 1989) on a rotatory shaker at 23°C under continuous irradiation with white light (55 μEinstein m^{-2} s^{-1}). To test the sensitivity of algal strains to $^1O_2$, 1.5×10^3 and 3×10^4 cells were spotted in three replicates on an agar plate containing 2 μM of the photosensitizer MB (Merck) and incubated for 6 h under HL (1000 μE m^{-2} s^{-1}), followed by recovery in normal light (55 μE m^{-2} s^{-1}) for 20 d.

Insertional Mutagenesis and Screening for $^1O_2$ Mutants in *C. reinhardtii*

To produce insertional mutants for screening, a *C. reinhardtii* strain harboring the $^1O_2$-inducible *G. princeps* luciferase cassette (Shao and Bock, 2008) was transformed with a 1.7-kb *Hin*dIII restriction fragment carrying the P_{TUB}:*aph7″* hygromycin resistance cassette from vector pHyg3 (Berthold et al., 2002). To this end, samples of 10^8 cells were transformed with 30 ng of fragment DNA using the glass bead–assisted transformation method (Kindle, 1990; Neupert et al., 2012). Transformants were selected on TAP plates containing 10 μg/mL of hygromycin B. For $^1O_2$ induction of reporter gene expression, transgenic colonies grown for 2 weeks on TAP plates in continuous light (55 μE m^{-2} s^{-1}) at 23°C were resuspended in 50 μL of TAP medium with or without 1 μM MB in 96-well microtiter plates and treated with HL (1000 μE m^{-2} s^{-1}) for 1 h. After recovery in normal light for 3 to 4 h at room temperature, bioluminescence of the samples was measured with a luminometer (MicroBeta TriLux; Shao and Bock, 2008), and the fold induction of luciferase activity was calculated by comparison with the control sample not exposed to HL treatment. To monitor heat shock induction of luciferase expression, luminescence images of algal colonies were recorded with an ultrasensitive photon-counting camera (Hamamatsu) after shifting the culture plates from 23 to 40°C for 1 h and recovery at room temperature for 1 h (Shao and Bock, 2008).

Construction of Transformation Vectors for *C. reinhardtii*

The reading frame of the *MBS* gene from *C. reinhardtii* (Cr-*MBS*) was amplified with or without its stop codon by PCR using the EST clone AV621044 as a template and specific primers (primer NdeI-ZF combined with ZF-EcoRI or ZF-SnaBEcoRI; see Supplemental Table 1 online). The P_{PsaD}:*MBS* construct was cloned by inserting the Cr-*MBS* fragment with the stop codon as *Nde*I/*Eco*RI restriction fragment into the Cr-*PsaD* expression cassette (Fischer and Rochaix, 2001) of a vector harboring the paromomycin resistance gene *aphVIII* as selectable marker gene (Sizova et al., 2001). To produce an *MBS-YFP* fusion gene, the Cr-*MBS* fragment lacking the stop codon and containing an additional *Sna*BI site at the 3′ end was inserted into the *PsaD* expression cassette. Subsequently, a PCR-amplified *YFP* fragment with *Sna*BI-*Eco*RI ends (see Supplemental Table 1 online) was integrated between Cr-*MBS* and the *PsaD* terminator, generating the P_{PsaD}:*MBS-YFP* expression construct.

Isolation of Genomic DNA from *C. reinhardtii* and Identification of Insertion Sites by Inverse PCR

Total genomic DNA from *C. reinhardtii* was extracted following published protocols (Schroda et al., 2001). Inverse PCR was performed according to standard procedures (Jong et al., 2002) with the modification that nested PCRs were performed. Briefly, 0.5- to 1-μg aliquots of genomic DNA were digested overnight with either *Pst*I or *Puv*II at 37°C in a total volume of 50 μL. Following phenol extraction and ethanol precipitation, self-ligation by T4 DNA ligase was performed with 100 ng of purified DNA in a 100-μL reaction volume overnight at 4°C. The ligated DNA was then linearized by digestion with *Sac*I, a restriction enzyme with a unique cleavage site in the P_{TUB}:*aph7″* expression cassette. The purified *Sac*I-digested DNA was used in inverse PCR reactions with the primers Inv-Hyg-f and Inv-Hyg-r (see Supplemental Table 1 online). Nested PCR with primers LMS-Hyg-f and LMS-Hyg-r amplified the insertion site-specific band and, in the case of the P45E1 mutant (*mbs* mutant), gave a band of ~2.5 kb that was purified from the agarose gel and sequenced. The sequences flanking the insertion site were extracted from the *C. reinhardtii* genome sequence (Joint Genome Initiative version 4.0; Merchant et al., 2007) and analyzed with respect to the predicted gene models. Specific primers for Cr-*MBS* (see Supplemental Table 1) were designed according to the sequence of EST clone AV621044.

Transformation of *C. reinhardtii*

Nuclear transformation of *C. reinhardtii* was performed using the glass bead method (Kindle, 1990). For complementation of the *mbs* mutant, 200 ng of linearized DNA of the P_{PsaD}:*MBS* plasmid was transformed and transgenic strains were selected on agar-solidified TAP medium containing

10 μg/mL of paromomycin. Transformants were screened for their luciferase activity in response to $^1O_2$ induction with 1 μM MB in HL (1000 μE m^{-2} s^{-1}) for 1 h. To determine the subcellular localization of MBS, the linearized P_{PsaD}:*MBS-YFP* plasmid was transformed into *C. reinhardtii* expression strain UVM11 (Neupert et al., 2009) followed by selection of transformants for paromomycin resistance.

Arabidopsis thaliana Lines, Growth Conditions, and Stress Treatments

Arabidopsis wild-type and mutant plants (all ecotype Columbia) were grown on half-strength Murashige and Skoog medium (Murashige and Skoog, 1962) with 1% Suc for 12 d and then transferred to soil and cultivated under long-day conditions (16 h light/8 h dark, 22°C/18°C) at a light intensity of 120 μE m^{-2} s^{-1}. HL stress treatments were performed under 900 to 1100 μE m^{-2} s^{-1} (16 h light/8 h dark) at 21°C and 55% relative humidity. Prior to HL stress treatments, plants were incubated in low light (10 to 20 μE m^{-2} s^{-1}) for 7 d. The T-DNA insertion lines *mbs1-1* (SAIL_661_B05), *mbs1-2* (WiscDsLox337D07), and *mbs2-1* (SALK_091719) were obtained from the Nottingham Arabidopsis Stock Centre. Homozygous T-DNA lines were identified by PCR using genomic DNA and T-DNA–specific primers (LB-SALK-b1.3, LB-Wisc, and LB-SAIL) in combination with gene-specific primers (see Supplemental Table 2 online). All PCR products were sequenced to confirm the T-DNA insertions. The *Arabidopsis flu* mutant (op den Camp et al., 2003) was grown from seeds in continuous light.

Plant Transformation Constructs and Generation of Stable Transgenic *Arabidopsis* Lines

The RNAi-*MBS1* and RNAi-*MBS2* vectors were constructed using gene-specific tags of *MBS1* (pENTR207_CATMA3a01730) and *MBS2* (pENTR207_CATMA5a14770) from the AGRIKOLA collection of RNAi vectors (Hilson et al., 2004; Figure 2A; see Supplemental Table 3 online). The gene-specific tag region of the entry clones was recombined into the RNAi vector pK7GWIWG2(I) (Karimi et al., 2002). To generate the *35S:MBS1* overexpression construct, the PCR-amplified *MBS1* reading frame was inserted into a CaMV 35S expression cassette as a *Bam*HI-*Xba*I fragment (for sequences of PCR primers BamH-3g02790 and At3g02790-XbaI, see Supplemental Table 4 online). To construct a transformation vector for expression of an MBS1-GFP fusion protein (P_{MBS1}:*MBS1-GFP* construct), a 1252-bp fragment covering the region upstream of the *MBS1* start codon and the *MBS1* reading frame without its stop codon (obtained by PCR with primers SacI-3g02790 and At3g02790-NcoI followed by digestion with *Sac*I and *Nco*I; see Supplemental Table 4 online) was ligated to the coding region of *GFP* followed by the octopine synthase terminator. Transformation of wild-type plants and *mbs1-1* mutant plants was performed by the floral dip method (Clough and Bent, 1998) using *Agrobacterium tumefaciens* strain GV3101:pMP90:pSOUP.

Subcellular Localization and Microscopy Analyses

GFP fusion constructs of the full-length coding regions of At-*MBS1* and At-*MBS2* were transiently expressed in tobacco (*Nicotiana tabacum*) protoplasts by polyethylene glycol–mediated DNA uptake. To this end, the At-*MBS* genes were PCR amplified with gene-specific primers introducing restriction sites for *Xho*I and *Nco*I at the 5′ and 3′ ends, respectively (see Supplemental Table 4 online). After digestion with *Xho*I and *Nco*I, the amplification products were ligated to the *GFP* gene in vector pA7-GFP (Voelker et al., 2006), generating an in-frame translational fusion between the *MBS* gene and the coding sequence of *GFP* under the control of the CaMV 35S promoter. For subcellular localization analyses, plasmids were transiently transformed into tobacco protoplasts (Huang et al., 2002). To test for colocalization with PBs and SGs, the pA7-MBS1-GFP vector was cotransformed with the Dcp1 or Rbp47 reporter constructs (Weber et al., 2008) into protoplasts. $^1O_2$ stress treatments were performed under HL in the presence of 1 μM MB for 30 min. Subcellular localization of reporter protein fluorescence was determined by confocal laser scanning microscopy (Leica TCS SP5) using a HCx PL APO ×63 W objective lens. Excitation wavelengths were 488 nm for GFP, 514 nm for YFP, 561 nm for RFP, and 488 nm for chlorophyll fluorescence.

Isolation of Nucleic Acids, cDNA Synthesis, and RT-PCR

Total plant DNA was isolated from fresh leaf material by a rapid mini-prep procedure (Doyle and Doyle, 1990). Total cellular RNA was extracted using the peqGold TriFast reagent (Peqlab). RNA samples were digested with DNase (TURBO DNA-free kit; Ambion), and cDNA was synthesized using SuperScript III reverse transcriptase (Invitrogen) and oligo$(dT)_{18}$ primers according to the manufacturer's instructions (for RT-PCR primers, see Supplemental Table 5 online). cDNAs from *C. reinhardtii* were amplified using TaKaRa LA Taq polymerase with GC buffer (Fisher Scientific) and specific primers (see Supplemental Table 5 online) under the following conditions: 94°C for 2 min, 30 cycles of 94°C for 30 s, 60°C for 1 min, and 72°C for 30 s, followed by a final extension at 72°C for 5 min. For qRT-PCR analyses in *Arabidopsis*, *Actin2* or *Ubi10* were amplified as controls for cDNA quality. For the analysis of stress-responsive gene expression by qRT-PCR, 12-d-old *Arabidopsis* seedlings grown on agar plates and adapted to 10 μE m^{-2} s^{-1} continuous light for 7 d were exposed to HL stress (1000 μE m^{-2} s^{-1}, followed by a 3-h dark period), and samples were collected at different time points. qRT-PCR assays were performed using the LightCycler 480 real-time PCR system (Roche Applied Science) and Absolute SYBR Green ROX mix (Thermo Scientific; for primers, see Supplemental Table 6 online). mRNA abundance of stress-related genes was normalized to the *Profilin1* (At2g19760; Baruah et al., 2009) expression level. To confirm the suitability of *Profilin1* as reference gene under light stress, the expression of *CYP5* (At2g29960) was analyzed as an additional reference. The reference genes changed by ≤1.2 cycles under the conditions of our light stress experiments for initial qRT-PCR evaluation of stress marker gene expression and by ≤0.5 cycles in the light stress experiment used for microarray analysis (see below). Three biological replicates were analyzed with two technical replicates each. The $2^{-\Delta\Delta CT}$ (cycle threshold) method was used to determine relative transcript levels (Livak and Schmittgen, 2001). Statistical evaluation was performed by analysis of variance with Microsoft Office Excel 2010. Nonquantitative RT-PCR with *Arabidopsis* cDNAs was performed under the following conditions: 94°C for 2 min, 30 cycles of 94°C for 30 s, 50°C for 1 min, and 72°C for 30 s, followed by a final extension at 72°C for 5 min. For primer sequences, see Supplemental Table 5 online.

Expression of Recombinant At-MBS1 Protein and Generation of Anti-At-MBS1 Antibodies

To generate a vector for overexpression of At-*MBS1* in *Escherichia coli*, the reading frame was amplified with gene-specific primers (NdeI-At3g02790 and At3g02790EcoRI; see Supplemental Table 4 online), introducing restriction sites for *Nde*I and *Eco*RI at the 5′ and 3′ end, respectively. The PCR product was digested with *Nde*I and *Eco*RI and ligated into expression vector pET21b (Novagene). Polyclonal anti-MBS1 antibodies were produced by immunizing rabbits (BioGenes) with purified At-MBS1 protein overexpressed in *E. coli*.

To test for a possible $^1O_2$-scavenging function of MBS proteins in *E. coli*, Cr-*MBS* and At-*MBS1* were overexpressed from pET vectors. As a control, a strain overexpressing a short fragment of ovalbumin (amino acids 280 to 362) was used. Protein expression was induced by addition of 0.1 mM isopropyl-β-D-thiogalactopyranosid to the cultures (at OD_{600} = 0.6) followed by incubation for 2 h at room temperature. $^1O_2$ stress tolerance

was analyzed by comparing the growth of the strains on Luria-Bertani medium containing 5 μM MB and release of $^1O_2$ by light treatment (at 1000 μE m^{-2} s^{-1} for 4 h). A dilution series of cultures spotted onto the Luria-Bertani agar plates with or without MB was analyzed in triplicate.

Protein Isolation and Protein Gel Blots

Total plant protein was extracted using a phenol-based method described previously (Petersen and Bock, 2011). Protein extracts were electrophoretically separated in Tricine-SDS polyacrylamide gels (Schägger and von Jagow, 1987) and transferred to Hybond-P polyvinylidene difluoride membranes (GE Healthcare) using a Trans-Blot cell (Bio-Rad) and a standard transfer buffer (192 mM Gly, 25 mm Tris, 20% methanol, and 2% SDS, pH 8.3). Immunoblot detection was performed with specific antibodies using the enhanced chemiluminescence system (ECL PLUS; GE Healthcare). Polyclonal antibodies against the O-subunit of photosystem II and a peroxidase-conjugated anti-rabbit IgG were purchased from Agrisera.

Enrichment of RNA Granules and RNase Treatment

Four-week-old plants grown in soil were treated with HL (1000 μE m^{-2} s^{-1}) for 3 h and then transferred to the normal light (120 μE m^{-2} s^{-1}) for 45 min. The leaves were harvested, quickly ground at 4°C, and then lysed by rotation in the presence of cold lysis buffer composed of 1% Triton X-100, 0.4 mM Tris, pH 7.5, 5 mM NaCl, 6.25 mM $MgCl_2$, 10 μM DTT, and 1× protease inhibitor cOmplete Mini EDTA free (Roche). Lysis was performed for 15 min at 4°C in the presence or absence of 0.4 units/μL of RNase inhibitor. Lysates were cleared by brief centrifugation at 2000*g* for 2 min at 4°C. The supernatant was centrifuged at 10,000*g* for 10 min at 4°C, yielding a pellet of semipurified PBs (Teixeira et al., 2005). To test for RNA sensitivity, the resuspended pellet was treated with RNase A (1 μg/μL for 10 min at room temperature; Teixeira et al., 2005). For microscopy analysis, 5 μL of the PB-enriched pellet was examined directly with the confocal microscope.

Imaging of H_2O_2 and $^1O_2$ in *Arabidopsis* Leaves

Detection of H_2O_2 and $^1O_2$ by staining of intact leaves with diamino benzidine and SOSG, respectively, was performed according to published protocols (Driever et al., 2009). For SOSG imaging, 12-d-old *Arabidopsis* seedlings were vacuum infiltrated with 100 μM SOSG in the dark and then exposed to HL (1000 μE m^{-2} s^{-1}) for 1 h, while the control plants were kept in the dark. SOSG fluorescence images were taken with a confocal laser scanning microscope (Leica TCS SP5; excitation at 496 nm) or a fluorescence stereomicroscope (Leica MZ16 FA; excitation at 470/510 nm).

Determination of Anthocyanin and Chlorophyll Contents and Chlorophyll Fluorescence Measurements

Determination of chlorophyll and anthocyanin contents in *Arabidopsis* leaves was performed following published protocols (Lichtenthaler, 1987; Lohmann et al., 2006). Chlorophyll *a* fluorescence was recorded using a pulse-amplitude modulated fluorometer (DUAL-PAM-100; Heinz Walz) on intact plants at room temperature as described previously (Schöttler et al., 2007a, 2007b). Plants were dark-adapted for 15 min prior to determination of the maximum photochemical efficiency of PSII (F_v/F_m). PSII photoinhibition was measured by the decrease in the chlorophyll fluorescence ratio F_v/F_m in detached leaves exposed to HL stress (1000 μE m^{-2} s^{-1}) for 4 h followed by recovery at low light (20 μE m^{-2} s^{-1}) for 4 h.

Microarray Experiments

Light stress–regulated gene expression profiles were analyzed with Affymetrix ATH1 microarrays. Five *Arabidopsis* genotypes were compared: the wild type, *mbs1-1*, *RNAi-MBS2 mbs1-1*, *35S:MBS1*, and the *flu* mutant (op den Camp et al., 2003). Twelve-day-old *Arabidopsis* seedlings grown on agar plates with half-strength Murashige and Skoog medium (supplemented with 1% Suc) and adapted to 10 μE m^{-2} s^{-1} continuous light for 7 d. Following a 3-h dark period, seedlings were exposed to HL stress (1000 μE m^{-2} s^{-1}). The leaves were immediately collected at 0 h (time point HL 0 h) and 3 h (HL 3 h) of light stress. Three biological replicates were analyzed for each time point.

Total cellular RNA was extracted using the NucleoSpin RNA Plant kit (Macherey-Nagel) according to the manufacturer's instructions, without DNase digestion. The remaining DNA was digested using the Ambion DNA-free DNase Treatment and Removal Reagents (Invitrogen). RNA quality and quantity of samples were determined by analysis on an Agilent 2100 Bioanalyzer using the Agilent RNA 6000 Nano kit (Agilent Technologies). Transcript profiles were analyzed with Affymetrix GeneChip ATH1 arrays (ATLAS Biolabs). Raw data were passed through quality assessment and statistical analysis using Robin (Lohse et al., 2010) and the R software package (http://www.r-project.org). Each array was background-adjusted and normalized by the robust multiarray average normalization method in the R package "affy" (Irizarry et al., 2003). For each probe, the average expression level of the three replicates was calculated. Microarray data sets were deposited in the National Center for Biotechnology Information Gene Expression Omnibus database (accession number GSE49596; http://www.ncbi.nlm.nih.gov/geo/query/acc.cgi?acc=GSE49596).

Arabidopsis genes specifically responding to $^1O_2$ or H_2O_2/O_2^- were selected based on two previously published comprehensive studies on ROS signaling that also used Affymetrix ATH1 microarrays for transcript profiling (op den Camp et al., 2003; Gadjev et al., 2006; see Supplemental Data Set 1 online). To determine differentially expressed genes, $\log_2$-fold changes (HL 3 h/HL 0 h) were calculated for each probe set on the Affymetrix ATH1 array and each genotype. Genes whose P value was ≤0.05 and whose absolute value of $\log_2$-fold change (HL 3 h/HL 0 h) was ≥2 were selected; among them, the genes known to be responsive to $^1O_2$ or H_2O_2/O_2^- (op den Camp et al., 2003; Gadjev et al., 2006) were identified (see Supplemental Data Set 2 online). False discovery rate correction (Benjamini and Hochberg, 1995) was performed by the function p.adjust in the R package "stats." Heat map was plotted using the heatmap.2 function in gplots of the R package. For clustering, hierarchical cluster analysis was used.

Accession Numbers

Sequence data from this article can be found in the Arabidopsis Genome Initiative or GenBank/EMBL databases under the following accession numbers: *Arabidopsis MBS1*, AT3G02790; *Arabidopsis MBS2*, AT5G16470; and *C. reinhardtii MBS*, jgi|Chlre4|298256.

Supplemental Data

The following materials are available in the online version of this article.

Supplemental Figure 1. Expression Patterns of *MBS1* and *MBS2* in Different Tissues and Developmental Stages of *Arabidopsis thaliana*.

Supplemental Figure 2. Phenotypic Analysis of Three Additional Complemented Lines of the *Arabidopsis mbs1-1* Mutant under High-Light Stress.

Supplemental Figure 3. At-MBS1 Localization to P-Bodies under $^1O_2$ Stress and RNase Sensitivity of MBS-Containing Cytosolic Granules.

Supplemental Figure 4. Production of Hydrogen Peroxide in Response to High-Light Stress in *Arabidopsis* Wild-Type Seedlings and the *mbs1-1* Mutant.

Supplemental Figure 5. Photosystem II Photoinhibition in Leaves of *Arabidopsis* Wild-Type Plants and *mbs1-1* Mutant Plants Exposed to High-Light Stress.

Supplemental Figure 6. Test for a Possible $^1O_2$-Scavenging Function of MBS Proteins in *E. coli*.

Supplemental Figure 7. Light Stress Response of Genes Previously Reported as Responsive to Reactive Oxygen Species.

Supplemental Figure 8. ROS-Responsive Genes That Are Significantly Changed in Their Expression under Light Stress in at Least One of the Plant Lines Analyzed.

Supplemental Figure 9. Quantitation of $^1O_2$ Accumulation in Leaves of the *Arabidopsis* Wild Type, the *mbs1-1* Mutant, and the *35S*:*MBS1*/*mbs1-1* Transgenic Line under Light Stress.

Supplemental Table 1. Oligonucleotides Used for *Chlamydomonas reinhardtii*.

Supplemental Table 2. Oligonucleotides for Genotyping of T-DNA Insertion Lines.

Supplemental Table 3. Transformation Vectors for the Generation of RNAi Lines and Their Gene-Specific Tags.

Supplemental Table 4. Oligonucleotides for Transgenic Constructs in *Arabidopsis*.

Supplemental Table 5. Oligonucleotides for RT-PCR.

Supplemental Table 6. Oligonucleotides for Quantitative Real-Time PCR.

Supplemental Data Set 1. List of Singlet Oxygen–Responsive and H_2O_2/O_2^--Responsive Genes and Their Regulation in the Wild Type, *mbs1-1*, *RNAi-MBS2 mbs1-1*, *35S*:*MBS1*, and *flu* under Light Stress.

Supplemental Data Set 2. List of Singlet Oxygen–Responsive and H_2O_2/O_2^--Responsive Genes That Are Significantly Regulated under Light Stress in at Least One of the Plant Lines Analyzed (the Wild Type, *mbs1-1*, *RNAi-MBS2 mbs1-1*, *35S*:*MBS1*, and *flu*).

Supplemental Movie 1. Movie of the Trafficking of MBS1-Associated Cytoplasmic Foci under $^1O_2$ Stress.

ACKNOWLEDGMENTS

We thank Markus Fauth (University of Frankfurt) for plasmids carrying PB and SG marker genes and Klaus Apel (Boyce Thompson Institute, Cornell University) for providing seeds of the *flu* mutant. We thank Michael Schroda (University of Kaiserslautern), Eric Lam (Rutgers University), Takuya Matsuo (Nagoya University), Jean-David Rochaix (University of Geneva), Klaus Apel, and Wenbin Zhou (Max-Planck-Institut für Molekulare Pflanzenphysiologie) for helpful discussions. We thank Eugenia Maximova for discussion and help with microscopy, Wenbin Zhou and Mark A. Schöttler for help with chlorophyll fluorescence measurements, Frederik Sommer for help with protein purification, and Annemarie Matthes and Christin Albus (all Max-Planck-Institut für Molekulare Pflanzenphysiologie) for help with optimizing MBS protein detection. This work was supported by grants from the Bundesministerium für Bildung und Forschung (Systems Biology Initiative FORSYS) and the Deutsche Forschungsgemeinschaft (FOR 804; BO 1482/15-2) to R.B.

AUTHOR CONTRIBUTIONS

N.S. designed and performed research, analyzed data, and provided input on the article. G.Y.D. analyzed data. R.B. designed research, analyzed data, and wrote the article.

Received August 14, 2013; revised August 14, 2013; accepted September 30, 2013; published October 22, 2013.

REFERENCES

Adhikari, N.D., Froehlich, J.E., Strand, D.D., Buck, S.M., Kramer, D.M., and Larkin, R.M. (2011). GUN4-porphyrin complexes bind the ChlH/GUN5 subunit of Mg-Chelatase and promote chlorophyll biosynthesis in *Arabidopsis*. Plant Cell **23:** 1449–1467.

Antoni, R., Rodriguez, L., Gonzalez-Guzman, M., Pizzio, G.A., and Rodriguez, P.L. (2011). News on ABA transport, protein degradation, and ABFs/WRKYs in ABA signaling. Curr. Opin. Plant Biol. **14:** 547–553.

Apel, K., and Hirt, H. (2004). Reactive oxygen species: Metabolism, oxidative stress, and signal transduction. Annu. Rev. Plant Biol. **55:** 373–399.

Baruah, A., Simková, K., Apel, K., and Laloi, C. (2009). *Arabidopsis* mutants reveal multiple singlet oxygen signaling pathways involved in stress response and development. Plant Mol. Biol. **70:** 547–563.

Benjamini, Y., and Hochberg, Y. (1995). Controlling the false discovery rate: A practical and powerful approach to multiple testing. J. R. Stat. Soc. B **57:** 289–300.

Berthold, P., Schmitt, R., and Mages, W. (2002). An engineered *Streptomyces hygroscopicus* aph 7′′ gene mediates dominant resistance against hygromycin B in *Chlamydomonas reinhardtii*. Protist **153:** 401–412.

Brzezowski, P., Wilson, K.E., and Gray, G.R. (2012). The PSBP2 protein of *Chlamydomonas reinhardtii* is required for singlet oxygen-dependent signaling. Planta **236:** 1289–1303.

Clough, S.J., and Bent, A.F. (1998). Floral dip: A simplified method for Agrobacterium-mediated transformation of *Arabidopsis thaliana*. Plant J. **16:** 735–743.

Coll, N.S., Danon, A., Meurer, J., Cho, W.K., and Apel, K. (2009). Characterization of soldat8, a suppressor of singlet oxygen-induced cell death in *Arabidopsis* seedlings. Plant Cell Physiol. **50:** 707–718.

Dent, R.M., Haglund, C.M., Chin, B.L., Kobayashi, M.C., and Niyogi, K.K. (2005). Functional genomics of eukaryotic photosynthesis using insertional mutagenesis of *Chlamydomonas reinhardtii*. Plant Physiol. **137:** 545–556.

Doyle, J.J., and Doyle, J.L. (1990). Isolation of plant DNA from fresh tissue. Focus **12:** 13–15.

Driever, S.M., Fryer, M.J., Mullineaux, P.M., and Baker, N.R. (2009). Imaging of reactive oxygen species in vivo. Methods Mol. Biol. **479:** 109–116.

Du, Y.-Y., Wang, P.-C., Chen, J., and Song, C.-P. (2008). Comprehensive functional analysis of the catalase gene family in *Arabidopsis thaliana*. J. Integr. Plant Biol. **50:** 1318–1326.

Finkel, T. (2011). Signal transduction by reactive oxygen species. J. Cell Biol. **194:** 7–15.

Fischer, B.B., Eggen, R.I., and Niyogi, K.K. (2010). Characterization of singlet oxygen-accumulating mutants isolated in a screen for altered oxidative stress response in *Chlamydomonas reinhardtii*. BMC Plant Biol. **10:** 279.

Fischer, B.B., Krieger-Liszkay, A., Hideg, É., Snyrychová, I., Wiesendanger, M., and Eggen, R.I.L. (2007). Role of singlet oxygen in chloroplast to nucleus retrograde signaling in *Chlamydomonas reinhardtii*. FEBS Lett. **581:** 5555–5560.

Fischer, B.B., Ledford, H.K., Wakao, S., Huang, S.G., Casero, D., Pellegrini, M., Merchant, S.S., Koller, A., Eggen, R.I.L., and Niyogi, K.K. (2012). SINGLET OXYGEN RESISTANT 1 links reactive electrophile signaling to singlet oxygen acclimation in *Chlamydomonas reinhardtii*. Proc. Natl. Acad. Sci. USA **109:** E1302–E1311.

Fischer, N., and Rochaix, J.-D. (2001). The flanking regions of PsaD drive efficient gene expression in the nucleus of the green alga *Chlamydomonas reinhardtii*. Mol. Genet. Genomics **265:** 888–894.

Foyer, C.H., and Noctor, G. (2003). Redox sensing and signalling associated with reactive oxygen in chloroplasts, peroxisomes and mitochondria. Physiol. Plant. **119:** 355–364.

Gadjev, I., Vanderauwera, S., Gechev, T.S., Laloi, C., Minkov, I.N., Shulaev, V., Apel, K., Inzé, D., Mittler, R., and Van Breusegem, F.

(2006). Transcriptomic footprints disclose specificity of reactive oxygen species signaling in Arabidopsis. Plant Physiol. **141:** 436–445.

Galvez-Valdivieso, G., Fryer, M.J., Lawson, T., Slattery, K., Truman, W., Smirnoff, N., Asami, T., Davies, W.J., Jones, A.M., Baker, N.R., and Mullineaux, P.M. (2009). The high light response in *Arabidopsis* involves ABA signaling between vascular and bundle sheath cells. Plant Cell **21:** 2143–2162.

Galvez-Valdivieso, G., and Mullineaux, P.M. (2010). The role of reactive oxygen species in signalling from chloroplasts to the nucleus. Physiol. Plant. **138:** 430–439.

Gill, S.S., and Tuteja, N. (2010). Reactive oxygen species and antioxidant machinery in abiotic stress tolerance in crop plants. Plant Physiol. Biochem. **48:** 909–930.

Gonzalez-Ballester, D., Pootakham, W., Mus, F., Yang, W., Catalanotti, C., Magneschi, L., de Montaigu, A., Higuera, J.J., Prior, M., Galván, A., Fernandez, E., and Grossman, A.R. (2011). Reverse genetics in Chlamydomonas: A platform for isolating insertional mutants. Plant Methods **7:** 24.

Harris, E.H. (1989). The Chlamydomonas Sourcebook. (San Diego, CA: Academic Press).

Henmi, T., Miyao, M., and Yamamoto, Y. (2004). Release and reactive-oxygen-mediated damage of the oxygen-evolving complex subunits of PSII during photoinhibition. Plant Cell Physiol. **45:** 243–250.

Hilson, P., et al. (2004). Versatile gene-specific sequence tags for *Arabidopsis* functional genomics: Transcript profiling and reverse genetics applications. Genome Res. **14** (10B)**:** 2176–2189.

Huang, F.-C., Klaus, S.M.J., Herz, S., Zou, Z., Koop, H.-U., and Golds, T.J. (2002). Efficient plastid transformation in tobacco using the aphA-6 gene and kanamycin selection. Mol. Genet. Genomics **268:** 19–27.

Irizarry, R.A., Hobbs, B., Collin, F., Beazer-Barclay, Y.D., Antonellis, K.J., Scherf, U., and Speed, T.P. (2003). Exploration, normalization, and summaries of high density oligonucleotide array probe level data. Biostatistics **4:** 249–264.

Jaspers, P., and Kangasjärvi, J. (2010). Reactive oxygen species in abiotic stress signaling. Physiol. Plant. **138:** 405–413.

Jiang, C., Belfield, E.J., Mithani, A., Visscher, A., Ragoussis, J., Mott, R., Smith, J.A.C., and Harberd, N.P. (2012). ROS-mediated vascular homeostatic control of root-to-shoot soil Na delivery in *Arabidopsis*. EMBO J. **31:** 4359–4370.

Jong, A.Y., T'ang, A., Liu, D.P., and Huang, S.H. (2002). Inverse PCR. Genomic DNA cloning. Methods Mol. Biol. **192:** 301–307.

Karcher, D., Köster, D., Schadach, A., Klevesath, A., and Bock, R. (2009). The Chlamydomonas chloroplast HLP protein is required for nucleoid organization and genome maintenance. Mol. Plant **2:** 1223–1232.

Karimi, M., Inzé, D., and Depicker, A. (2002). GATEWAY vectors for Agrobacterium-mediated plant transformation. Trends Plant Sci. **7:** 193–195.

Kim, C., Lee, K.P., Baruah, A., Nater, M., Göbel, C., Feussner, I., and Apel, K. (2009). ($^{1}O_2$-mediated retrograde signaling during late embryogenesis predetermines plastid differentiation in seedlings by recruiting abscisic acid. Proc. Natl. Acad. Sci. USA **106:** 9920–9924.

Kim, C., Meskauskiene, R., Zhang, S., Lee, K.P., Lakshmanan Ashok, M., Blajecka, K., Herrfurth, C., Feussner, I., and Apel, K. (2012). Chloroplasts of *Arabidopsis* are the source and a primary target of a plant-specific programmed cell death signaling pathway. Plant Cell **24:** 3026–3039.

Kindle, K.L. (1990). High-frequency nuclear transformation of *Chlamydomonas reinhardtii*. Proc. Natl. Acad. Sci. USA **87:** 1228–1232.

Krieger-Liszkay, A., and Trebst, A. (2006). Tocopherol is the scavenger of singlet oxygen produced by the triplet states of chlorophyll in the PSII reaction centre. J. Exp. Bot. **57:** 1677–1684.

Lai, Z., Li, Y., Wang, F., Cheng, Y., Fan, B., Yu, J.Q., and Chen, Z. (2011). *Arabidopsis* sigma factor binding proteins are activators of the WRKY33 transcription factor in plant defense. Plant Cell **23:** 3824–3841.

Laloi, C., Stachowiak, M., Pers-Kamczyc, E., Warzych, E., Murgia, I., and Apel, K. (2007). Cross-talk between singlet oxygen- and hydrogen peroxide-dependent signaling of stress responses in *Arabidopsis thaliana*. Proc. Natl. Acad. Sci. USA **104:** 672–677.

Lam, E. (2008). Programmed cell death in plants: Orchestrating an intrinsic suicide program within walls. Crit. Rev. Plant Sci. **27:** 413–423.

Lam, E., Kato, N., and Lawton, M. (2001). Programmed cell death, mitochondria and the plant hypersensitive response. Nature **411:** 848–853.

Lee, K.P., Kim, C., Landgraf, F., and Apel, K. (2007). EXECUTER1- and EXECUTER2-dependent transfer of stress-related signals from the plastid to the nucleus of *Arabidopsis thaliana*. Proc. Natl. Acad. Sci. USA **104:** 10270–10275.

Lichtenthaler, H.K. (1987). Chlorophylls and carotenoids: Pigments of photosynthetic biomembranes. Methods Enzymol. **148:** 350–382.

Liere, K., and Börner, T. (2007). Transcription and transcriptional regulation in plastids. Top. Curr. Genet. **19:** 121–174.

Livak, K.J., and Schmittgen, T.D. (2001). Analysis of relative gene expression data using real-time quantitative PCR and the 2(-ΔΔ C (T)) method. Methods **25:** 402–408.

Lodha, M., Schulz-Raffelt, M., and Schroda, M. (2008). A new assay for promoter analysis in Chlamydomonas reveals roles for heat shock elements and the TATA box in HSP70A promoter-mediated activation of transgene expression. Eukaryot. Cell **7:** 172–176.

Lohmann, A., Schöttler, M.A., Bréhélin, C., Kessler, F., Bock, R., Cahoon, E.B., and Dörmann, P. (2006). Deficiency in phylloquinone (vitamin K_1) methylation affects prenyl quinone distribution, photosystem I abundance, and anthocyanin accumulation in the *Arabidopsis* AtmenG mutant. J. Biol. Chem. **281:** 40461–40472.

Lohse, M., et al. (2010). Robin: An intuitive wizard application for R-based expression microarray quality assessment and analysis. Plant Physiol. **153:** 642–651.

Merchant, S.S., et al. (2007). The Chlamydomonas genome reveals the evolution of key animal and plant functions. Science **318:** 245–250.

Mittler, R., Vanderauwera, S., Suzuki, N., Miller, G., Tognetti, V.B., Vandepoele, K., Gollery, M., Shulaev, V., and Van Breusegem, F. (2011). ROS signaling: The new wave? Trends Plant Sci. **16:** 300–309.

Møller, I.M., and Sweetlove, L.J. (2010). ROS signalling—Specificity is required. Trends Plant Sci. **15:** 370–374.

Mubarakshina, M.M., Ivanov, B.N., Naydov, I.A., Hillier, W., Badger, M.R., and Krieger-Liszkay, A. (2010). Production and diffusion of chloroplastic H_2O_2 and its implication to signalling. J. Exp. Bot. **61:** 3577–3587.

Mullineaux, P., and Karpinski, S. (2002). Signal transduction in response to excess light: Getting out of the chloroplast. Curr. Opin. Plant Biol. **5:** 43–48.

Murashige, T., and Skoog, F. (1962). A revised medium for rapid growth and bio assays with tobacco tissue culture. Physiol. Plant. **15:** 473–497.

Neupert, J., Karcher, D., and Bock, R. (2009). Generation of Chlamydomonas strains that efficiently express nuclear transgenes. Plant J. **57:** 1140–1150.

Neupert, J., Shao, N., Lu, Y., and Bock, R. (2012). Genetic transformation of the model green alga *Chlamydomonas reinhardtii*. Methods Mol. Biol. **847:** 35–47.

op den Camp, R.G.L., Przybyla, D., Ochsenbein, C., Laloi, C., Kim, C., Danon, A., Wagner, D., Hideg, E., Göbel, C., Feussner, I., Nater, M., and Apel, K. (2003). Rapid induction of distinct stress responses after the release of singlet oxygen in *Arabidopsis*. Plant Cell **15:** 2320–2332.

Petersen, K., and Bock, R. (2011). High-level expression of a suite of thermostable cell wall-degrading enzymes from the chloroplast genome. Plant Mol. Biol. **76:** 311–321.

Pogson, B.J., Woo, N.S., Förster, B., and Small, I.D. (2008). Plastid signalling to the nucleus and beyond. Trends Plant Sci. **13:** 602–609.

Ramel, F., Birtic, S., Cuiné, S., Triantaphylidès, C., Ravanat, J.-L., and Havaux, M. (2012b). Chemical quenching of singlet oxygen by carotenoids in plants. Plant Physiol. **158:** 1267–1278.

Ramel, F., Birtic, S., Ginies, C., Soubigou-Taconnat, L., Triantaphylidès, C., and Havaux, M. (2012a). Carotenoid oxidation products are stress signals that mediate gene responses to singlet oxygen in plants. Proc. Natl. Acad. Sci. USA **109:** 5535–5540.

Ramel, F., Ksas, B., Akkari, E., Mialoundama, A.S., Monnet, F., Krieger-Liszkay, A., Ravanat, J.-L., Mueller, M.J., Bouvier, F., and Havaux, M. (2013b). Light-induced acclimation of the *Arabidopsis* chlorina1 mutant to singlet oxygen. Plant Cell **25:** 1445–1462.

Ramel, F., Mialoundama, A.S., and Havaux, M. (2013a). Nonenzymic carotenoid oxidation and photooxidative stress signalling in plants. J. Exp. Bot. **64:** 799–805.

Ramundo, S., Rahire, M., Schaad, O., and Rochaix, J.-D. (2013). Repression of essential chloroplast genes reveals new signaling pathways and regulatory feedback loops in *Chlamydomonas*. Plant Cell **25:** 167–186.

Schägger, H., and von Jagow, G. (1987). Tricine-sodium dodecyl sulfate-polyacrylamide gel electrophoresis for the separation of proteins in the range from 1 to 100 kDa. Anal. Biochem. **166:** 368–379.

Scheller, H.V., and Haldrup, A. (2005). Photoinhibition of photosystem I. Planta **221:** 5–8.

Schöttler, M.A., Flügel, C., Thiele, W., and Bock, R. (2007a). Knock-out of the plastid-encoded PetL subunit results in reduced stability and accelerated leaf age-dependent loss of the cytochrome b_6f complex. J. Biol. Chem. **282:** 976–985.

Schöttler, M.A., Flügel, C., Thiele, W., Stegemann, S., and Bock, R. (2007b). The plastome-encoded PsaJ subunit is required for efficient photosystem I excitation, but not for plastocyanin oxidation in tobacco. Biochem. J. **403:** 251–260.

Schroda, M., Blöcker, D., and Beck, C.F. (2000). The HSP70A promoter as a tool for the improved expression of transgenes in Chlamydomonas. Plant J. **21:** 121–131.

Schroda, M., Vallon, O., Whitelegge, J.P., Beck, C.F., and Wollman, F.-A. (2001). The chloroplastic GrpE homolog of *Chlamydomonas*: Two isoforms generated by differential splicing. Plant Cell **13:** 2823–2839.

Seo, M., and Koshiba, T. (2011). Transport of ABA from the site of biosynthesis to the site of action. J. Plant Res. **124:** 501–507.

Shao, N., and Bock, R. (2008). A codon-optimized luciferase from *Gaussia princeps* facilitates the in vivo monitoring of gene expression in the model alga *Chlamydomonas reinhardtii*. Curr. Genet. **53:** 381–388.

Shao, N., Krieger-Liszkay, A., Schroda, M., and Beck, C.F. (2007). A reporter system for the individual detection of hydrogen peroxide and singlet oxygen: Its use for the assay of reactive oxygen species produced in vivo. Plant J. **50:** 475–487.

Sizova, I., Fuhrmann, M., and Hegemann, P. (2001). A *Streptomyces rimosus* aphVIII gene coding for a new type phosphotransferase provides stable antibiotic resistance to *Chlamydomonas reinhardtii*. Gene **277:** 221–229.

Teixeira, D., Sheth, U., Valencia-Sanchez, M.A., Brengues, M., and Parker, R. (2005). Processing bodies require RNA for assembly and contain nontranslating mRNAs. RNA **11:** 371–382.

Tsukagoshi, H., Busch, W., and Benfey, P.N. (2010). Transcriptional regulation of ROS controls transition from proliferation to differentiation in the root. Cell **143:** 606–616.

Vanderauwera, S., Zimmermann, P., Rombauts, S., Vandenabeele, S., Langebartels, C., Gruissem, W., Inzé, D., and Van Breusegem, F. (2005). Genome-wide analysis of hydrogen peroxide-regulated gene expression in Arabidopsis reveals a high light-induced transcriptional cluster involved in anthocyanin biosynthesis. Plant Physiol. **139:** 806–821.

Voelker, C., Schmidt, D., Mueller-Roeber, B., and Czempinski, K. (2006). Members of the *Arabidopsis* AtTPK/KCO family form homomeric vacuolar channels in planta. Plant J. **48:** 296–306.

Wagner, D., Przybyla, D., Op den Camp, R., Kim, C., Landgraf, F., Lee, K.P., Würsch, M., Laloi, C., Nater, M., Hideg, E., and Apel, K. (2004). The genetic basis of singlet oxygen-induced stress responses of *Arabidopsis thaliana*. Science **306:** 1183–1185.

Weber, C., Nover, L., and Fauth, M. (2008). Plant stress granules and mRNA processing bodies are distinct from heat stress granules. Plant J. **56:** 517–530.